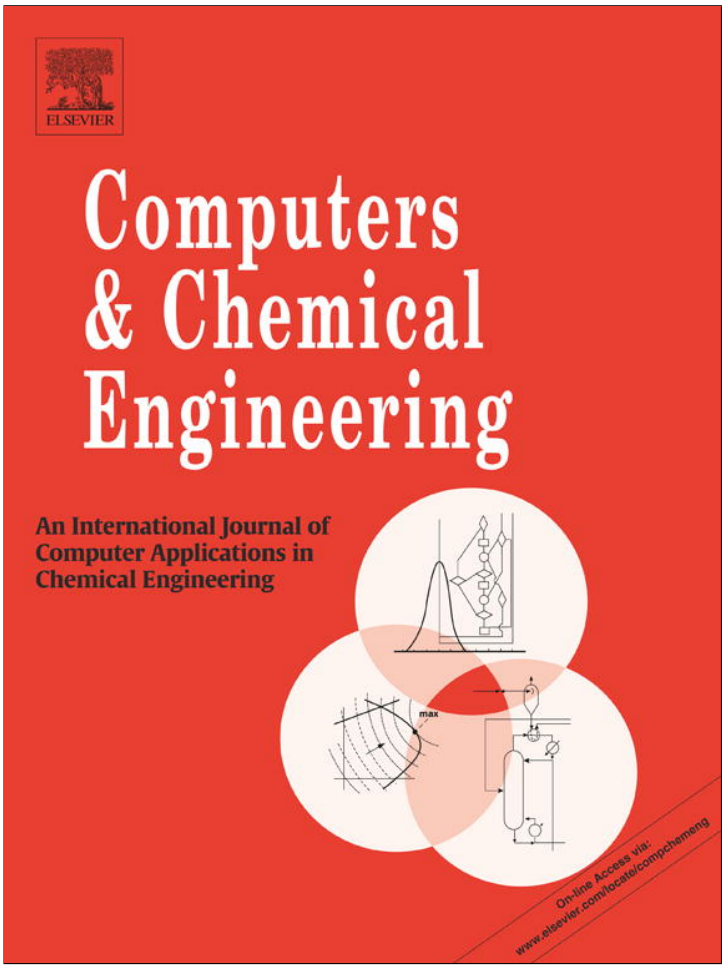

(This is a sample cover image for this issue. The actual cover is not yet available at this time.)

Computers and Chemical Engineering 50 (2013) 54–70

Contents lists available at SciVerse ScienceDirect

Computers and Chemical Engineering

journal homepage: www.elsevier.com/locate/compchemeng

Improvements on multiloop control design via net load evaluation

David Zumoffen[a,b,*], Marta Basualdo[a,b,c]

[a] Computer Aided for Process Engineering Group (CAPEG), French-Argentine International Center for Information and Systems Sciences (CIFASIS-CONICET-UNR-AMU), 27 de Febrero 210 bis, S2000EZP Rosario, Argentina
[b] Universidad Tecnológica Nacional – FRRo, Zeballos 1341, S2000BQA Rosario, Argentina
[c] Universidad Nacional de Rosario – FCEyA, Pellegrini 250, S2000BTP Rosario, Argentina

ARTICLE INFO

Article history:
Received 31 March 2012
Received in revised form 1 September 2012
Accepted 7 November 2012
Available online xxx

Keywords:
Plant-wide control
Disturbance rejection
Controllability
Sparse controller
Control structure design

ABSTRACT

The plant-wide control problem is a very important topic in process control. A particular control structure design will define (restrict) the future operability degree for the plant under study. Classical control policies (decentralized or full) are not always the best solution. In this context a systematic and generalized strategy to solve the multivariable plant-wide control problem is proposed here. The methodology called minimum square deviation (MSD) considers several points such as the optimal controlled variables (CVs) selection based on the sum of square deviation (SSD) and controller structure design supported by net load evaluation (NLE) analysis. The overall problem is combinatorial and is solved by accounting several steady-state tools and new indexes minimizing the heuristic load. Four well-known case studies are presented and other approaches taken from the literature are accounted for the sake of comparison. A robust stability test, μ-tools, is also performed for concluding about the control policies.

1. Introduction

The design strategies of industrial processes are generally focused on maximizing profits, optimizing energy use and ensure high standards on products. All these prerequisites normally produce highly coupled or interacting plants. Obviously, this is a good scenario from the profitability point of view, but a very challenging one from the plant-wide control perspective. This complexity increases with dimension, because large-scale processes could involve hundreds or thousands of variables to be considered. Hence, a control structure design (CSD) for guaranteeing the main process objectives is not a trivial task. Moreover, some process designs have serious problems to be solved because the lack of control information and evaluation at this stage. Generally, the process synthesis stage defines the connection between units, their sizing and the best operating conditions. This stage generally uses only steady-state (SS) information without considering issues such as optimal controlled variables (CVs) selection and controller structure design. It is crucial to identify some potential control problems at this phase for achieving a controllable plant design. However, only partial solutions exist to quantify these kinds of problems with SS tools only. Approaches having a good degree of both systematics and generalization are welcome, particularly when large-scale applications are involved. In this work a rigorous and generalized treatment of these aspects are proposed trying to avoid heuristic considerations for determining the final plant-wide control configuration.

Plant-wide CSD tasks involve CVs and MVs selection, input–output pairing definition, and controller structure design. Mainly the problem is solved by using process interaction measures. In some approaches a predefined CVs are used and the CSD problem dimension is reduced heuristically through the application of the engineering judgment (Buckley, 1964; Luyben, Tyréus, & Luyben, 1998). In this context, the relative gain array (RGA) approach, proposed by Bristol (1966), has been the preferred tool for decades and even today for developing more sophisticated approaches in plant-wide control area. This perhaps occurs because of its simplicity and effectiveness, although it is important to note that some publications have reported problems with RGA. In fact, several authors have been analyzed the RGA properties, its implications on control performance, and its drawbacks when the process is ill-conditioned or close to the singularity (Garcia & Morari, 1985; Grosdidier, Morari, & Holt, 1985; Skogestad & Postlethwaite, 2005; Skogetad & Morari, 1987). Other authors have proposed modifications to handle non-square process (Chang & Yu, 1990; Khaki-Sedigh & Moaveni, 2009; Skogestad & Postlethwaite, 2005), disturbances (Chang & Yu, 1992, 1994; Lin, Jeng, & Huang, 2009) and dynamic information (He, Cai, Ni, & Xie, 2009; McAvoy, Arkun, Chen, Robinson, & Schnelle, 2003). An excellent review of these techniques and new tendencies are given in Skogestad

* Corresponding author at: Computer Aided for Process Engineering Group (CAPEG), French-Argentine International Center for Information and Systems Sciences (CIFASIS-CONICET-UNR-AMU), 27 de Febrero 210 bis, S2000EZP Rosario, Argentina. Tel.: +54 341 4237248x332; fax: +54 341 482 1772.
E-mail addresses: zumoffen@cifasis-conicet.gov.ar (D. Zumoffen), basualdo@cifasis-conicet.gov.ar (M. Basualdo).

0098-1354/$ – see front matter © 2012 Elsevier Ltd. All rights reserved.
http://dx.doi.org/10.1016/j.compchemeng.2012.11.004

Nomenclature

Acronyms

CC	composition controller
CL	Chiang and Luyben
CS	control structure
CSD	control structure design
CVs	controlled variables
DVs	disturbances variables
EIP	error improvement percent
FOPD	first order plus delay
GA	genetic algorithms
GRDG	generalized relative disturbance array
IAE	integral absolute error
IMC	internal model control
LC	level controller
MIMO	multi-input/multi-output
MSD	minimum square deviation
MVs	manipulated variables
NRG	non-square relative gain
OMS	optimal manipulated selection
OR	Ogunnaike and Ray
PC	pressure controller
RGA	relative gain array
RNGA	relative normalized gain array
RS	robust stability
SS	steady-state
SSD	sum of squared deviations
SSV	structured singular value
TC	temperature controller
TFM	transference function matrix
UVs	uncontrolled variables

Variables

$\mathbf{A}(s)$	set point component – net load effect
$\mathbf{B}(s)$	disturbance component – net load effect
$\mathbf{d}_*(s)$	disturbance vector
$\mathbf{d}_*^p(i)$	ith-entry unitary vector
$\mathbf{D}(s)$	disturbance TFM
$\mathbf{D}_r(s)$	disturbance TFM for UVs
$\mathbf{D}_s(s)$	disturbance TFM for CVs
$\mathbf{F}(s)$	diagonal low pass TFM filter
$\mathbf{G}(s)$	process TFM
$\mathbf{G}_c(s)$	controller TFM
$\mathbf{G}_r(s)$	process TFM for UVs
$\mathbf{G}_r(s)$	process TFM for CVs
$\tilde{\mathbf{G}}_s(s)$	process model TFM for CVs
$\tilde{\mathbf{G}}_s^+(s)$	non-invertible TFM
$\tilde{\mathbf{G}}_{s\Gamma}(s)$	Process model TFM for Γ
$\tilde{\mathbf{G}}_{s\Gamma}^-(s)$	invertible process model TFM for Γ
$\mathbf{K}$	output feedback controller
$\mathbf{K}_N$	normalized process for RNGA
m	total outputs
n	total inputs
NLE_Γ	net load evaluation for Γ
p	total disturbances
$\mathbf{P}_s(s)$	nominal process
s	Laplace variable
SSD	sum of squared deviations index
t	time
$\mathbf{T}$	normalization matrix for RNGA
$\mathbf{u}(s)$	input vector
$\mathbf{y}(s)$	output vector
$\mathbf{y}_r(s)$	UVs vector
$\mathbf{y}_s(s)$	CVs vector
$\mathbf{y}_s^{net}(s)$	total net load effect
$\mathbf{y}_s^{sp}(s)$	set point vector
$\mathbf{y}_{sp}^n(i)$	ith-entry unitary vector

Greek symbols

γ	condition number
γ_{ij}	ij-component of Γ
Γ	parametrization matrix
Γ_{CY}	parametrization matrix proposed by Chang and Yu (1992)
Γ_{dS}	parametrization matrix proposed by Shen, Cai, and Li (2010)
Γ_f	full parametrization matrix
Γ_o	optimal parametrization matrix
Γ_{oS}	parametrization matrix proposed by Shen et al. (2010)
Δ_i	weight matrix, $i = 1, 2$
Θ_i	weight matrix, $i = 1, 2$
λ_i	ith eigenvalue
Λ_i	weight matrix, $i = 1, 2$
Λ_N	RNGA
μ_Δ	robust stability index
Ξ_i	weight matrix, $i = 1, 2$
$\underline{\sigma}$	minimum singular value
$\overline{\sigma}$	maximum singular value
τ_{fi}	ith filter time constant for $\mathbf{F}(s)$
ω	frequency

and Postlethwaite (2005) and Khaki-Sedigh and Moaveni (2009). Anyway, the plant-wide control problem is still an open problem and the continuous emergence of new strategies is a clear demonstration of this. In fact, a manipulated variables (MVs) selection approach by analyzing controllability for chemical process was presented in Yuan, Chen, and Zhao (2011). On the other hand, a new CVs selection approach based on both bidirectional branch and bound and local average loss is proposed by Kariwala and Cao (2010a). Moreover, a measurements selection criterion for steady-state indirect and self-optimizing control are proposed in Hori, Skogestad, and Alstad (2005) and Hori and Skogestad (2008). A systematic approach to design PID-based MIMO controller with different interaction levels (sparse controllers) is proposed in Shen et al. (2010) by using the new relative normalized gain array (RNGA) approach (He et al., 2009). An optimal control-based approach is presented (Assali & McAvoy, 2010) to determine a set of dominant measurements and MVs for improving both the production rate and product quality in the Tennessee Eastman (TE) process. These works show the efforts made by the scientific community and industry to improve both the way and the conditions for performing plant-wide control strategies.

Basically, the MSD procedure detailed here can be divided in two sequential combinatorial problems addressing the optimal CVs selection and the optimal controller structure design sequentially. The optimal CVs selection is based on sum of square deviations (SSD) index accounting both the operating point deviations of uncontrolled variables (UVs) and assuming the other output variables under perfect control. The controller structure design defines the input–output pairing and the controller interaction degree (sparse degree) based on the net load evaluation (NLE) index accounting references as well as disturbance effects on CVs. Note that, the sparse concept refers to the amount of components into the IMC approach, and directly related to the process model used. It is important to note that the SSD-based optimal CVs selection

is directly related with both, the non-square relative gain (NRG) array, suggested by Chang and Yu (1990) and perfect SS indirect control, proposed by Hori et al. (2005). But, in this work the NRG is generalized by using a new SSD scalar index avoiding a matrix analysis and including references effects. Moreover, the assumption of perfect control at SS is considered here to quantify deviations in UVs (not for inferential control or self-optimizing one). On the other hand, the NLE-based controller structure design proposed here is a generalization of the approach presented by Chang and Yu (1994) for synthesis of typical controller structures for robust load performance. Here, the new NLE scalar index allows to evaluate arbitrary controller structures (sparse) via internal model control (IMC) theory, reference changes and disturbance effects. The NLE-based controller design procedure also considers a stability/robustness test at steady-state (Garcia & Morari, 1985) to lead the search towards to feasible solutions set.

The MSD approach was tested partially (Zumoffen & Basualdo, 2009) (only the optimal CVs selection subroutine) and globally (Molina, Zumoffen, & Basualdo, 2011) (CV selection plus NLE) for a particular case study, the emblematic Tennessee Eastman process. This could be an isolated result closely related with this specific case study. The aim of this work is to demonstrate through other well-known benchmarks the real potentiality of the successful MSD procedure. In fact, the work proposed here presents a generalization of this approach through the following case studies: 2 non-square process as the Shell oil fractionator (Maciejowski, 2002) and the Newell and Lee evaporator (Govatsmark & Skogestad, 2001; Maciejowski, 2002), and 2 square plants the Ogunnaike and Ray (OR) (Luyben, 1986; Monica, Yu, & Luyben, 1988) and Chiang and Luyben (CL) (Chang & Yu, 1994) systems. In addition, illustrative examples are proposed to show some particular/additional matrix properties in the MSD procedure. All the controller structures proposed here are dynamically simulated and compared with other approaches available in the literature. Particularly, approaches proposed by Chang and Yu (1994) and Shen et al. (2010). Moreover, the improvements obtained with the MSD strategy are rigorously quantified by using the integral absolute tracking error (IAE) index for both, servo and regulator requirements. Finally, the robust stability conditions for all control policies and case studies are analyzed here. It is done based on the structured singular value (SSV) or μ procedure, accounting both, parametric and unmodeled dynamic uncertainties, for the closed-loop systems.

The main contributions of this work lie in: (A) generalize the SSD index via Frobenius norm for set point and disturbances effects, (B) give some mathematical insight about the SSD minimization tied to the selected subprocess properties, (C) integrate the NLE index for multivariable controller design with stability test, (D) NLE considering set point and disturbance effects, (E) MSD like a systematic and generalized tool for plant-wide control which minimizes the heuristic load, and (F) comparison with other approaches. Conclusions in Shen et al. (2010) are analyzed and compared.

2. The MSD approach for plant-wide control

The systematic and generalized minimum square deviation (MSD) procedure for performing plant-wide control proposed here is schematically represented in Fig. 1. The method addresses two important problems in control process in a unified framework: (1) the optimal CVs selection, represented through light gray blocks and (2) the controller structure design, dark gray blocks. Several

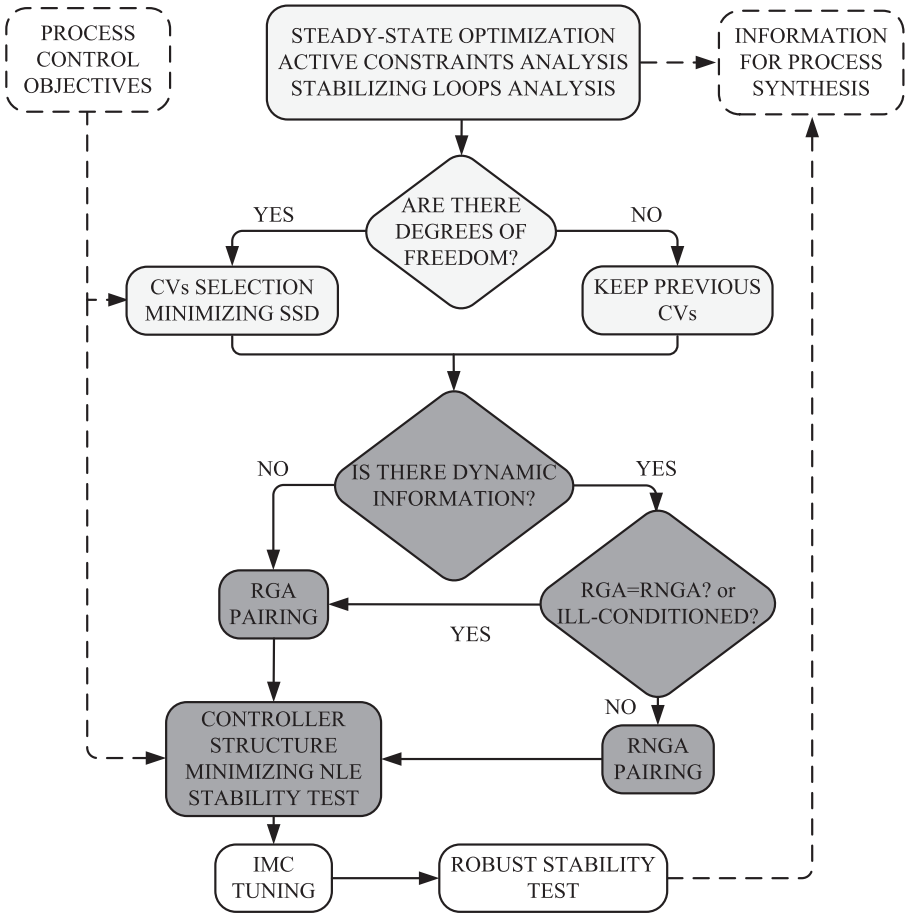

Fig. 1. MSD plant-wide control strategy.

tools and techniques are used in each subproblem which will be discussed below.

Assuming that the plant under study comes from the processes synthesis stage, then the information about the control objectives is not enough. So, the stability conditions of the plant must be analyzed. For unstable process, the minimum number of stabilizing control loops must be decided. After performing the process stabilization, a steady-state optimization analysis gives the optimum operating point by considering profit and safety. At this step some active constraints can be found which define some variables (measurements and manipulated) to necessarily be controlled (fixed), either by operating costs or stability issues. This first block still represents an open problem in plant-wide control (from generalized and systematic point of view). Anyway, in this work only stable processes or already stabilized plants are considered, so this block is not considered in detail.

The lines and blocks in dashed style in Fig. 1 represent information flow corresponding to partial control objectives into the MSD strategy (left) or information interchange with process synthesis stage (right). Note that partial control objectives refers to some a priori requisites, i.e. production rate, product quality, safety variables, etc. Information feedback between control performance and process synthesis is useful for improving both areas and obtain a successful plant design. In fact, the above integration is other open problem example in this field. Thus, information about product requirements, typical set point and disturbance magnitudes, relative degree of importance between outputs, etc. can be handled by assigning the corresponding weight matrices. The selection of the weights is a trade-off between controllability and synthesis proposals for a particular industrial process.

If there are no degrees of freedom, from the first block, then an optimal CVs selection is not necessary. Hence, the following step is the controller structure design procedure. On the other hand, if there are remaining degrees of freedom, the optimal CVs selection based on SSD index is proposed here. Basically, it is an optimization problem (combinatorial) which selects the best rows of the process by accounting the minimization of the SSD for uncontrolled variables (UVs) from their operational working point. Moreover, this approach also guarantees the well-conditioning of the selected subprocess to be controlled. This approach is addressed in detail in Section 2.1.

Once the above problem is solved, then the square subprocess is already defined. In this context, the next problem to solve is the input–output pairing and eventually the interaction degree of the controller structure. Dark gray blocks in Fig. 1 allow to perform these tasks in a generalized and systematic way. Specific details about the controller interaction degree approach is given in Section 2.2. Basically, a diagonal (base case) control structure is initially developed via the RGA or RNGA approaches. The selection between these methodologies is performed by analyzing both the dynamic information availability and the singularity degree of some matrices. Thus, by using this decentralized control policy, the controller interaction degree (sparse degree) is analyzed via minimization of the net load evaluation (NLE) scalar index, the stability constraint, and a suitable model parametrization. This can be done by a complete generalization of the net load effect ideas. This methodology is presented in detail in Section 2.2.

Finally, all control structures proposed by the MSD approach and classical ones (decentralized, full) can be compared via dynamic simulation. Hence, the last two blocks define the tuning for the controllers (IMC-based) and performing a rigorous robust stability analysis, respectively. The latter, based on structured singular value (SSV) theory or μ-analysis (Skogestad & Postlethwaite, 2005). Both parametric and unmodeled dynamic (multiplicative input) uncertainties were proposed for all delays and input gains of the processes respectively, generating a more realistic test environment for all control structures. Mathematical insights about the SSV approach are not presented here.

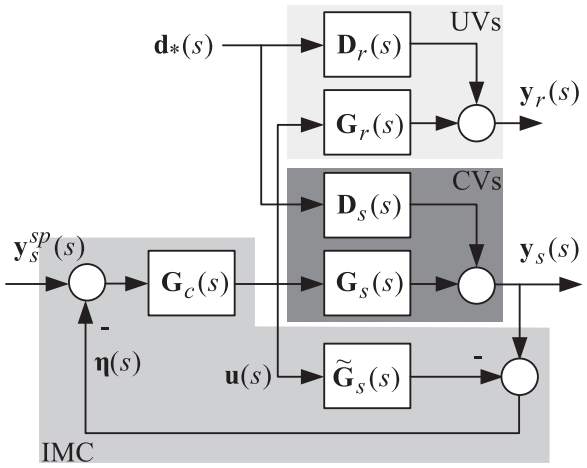

Fig. 2. Generalized IMC structure.

In the following both the optimal CVs selection and the CSD proposals are detailed together with the application results obtained through several illustrative and well-known examples.

2.1. Optimal CVs selection: SSD minimization

In this stage the remaining degrees of freedom, from the stabilization/optimization stage, are used for optimal CVs selection via a SSD philosophy. The aim is finding a subset of potential controlled variables to keep the process as close as possible to its desired operating point, i.e. uncontrolled variables (UVs) have minimal deviations at steady-state.

Assuming that the potential CVs are m and the available MVs are n with $m > n$, then $m - n$ degrees of freedom exist. Considering the process model in Laplace domain partitioned as

$$\mathbf{y}(s) = \mathbf{G}(s)\mathbf{u}(s) + \mathbf{D}(s)\mathbf{d}_*(s) = \begin{bmatrix} \mathbf{y}_r(s) \\ \mathbf{y}_s(s) \end{bmatrix} = \begin{bmatrix} \mathbf{G}_r(s) \\ \mathbf{G}_s(s) \end{bmatrix} \mathbf{u}(s) + \begin{bmatrix} \mathbf{D}_r(s) \\ \mathbf{D}_s(s) \end{bmatrix} \mathbf{d}_*(s) \quad (1)$$

where, $\mathbf{y}(s)$ is the total output vector, $\mathbf{y}_s(s)$ is the vector of selected CVs and $\mathbf{y}_r(s)$ is the UVs vector with dimensions $m \times 1$, $n \times 1$ and $(m-n) \times 1$ respectively. With $\mathbf{u}(s)$ corresponds to the available MVs vector of $n \times 1$ and $\mathbf{d}_*(s)$ the disturbances vector with $p \times 1$, being p the amount of considered disturbances. On the other hand, $\mathbf{G}_s(s)$ is a $n \times n$ transfer functions matrix (TFM) representing the input–output relationship for the CVs and $\mathbf{G}_r(s)$ is a $(m-n) \times n$ TFM containing the UVs (remaining variables). Similarly, $\mathbf{D}_s(s)$ and $\mathbf{D}_r(s)$ represent the disturbance models for each part of the process with dimensions $n \times p$ and $(m-n) \times p$ respectively. In this context, both the internal model control (IMC) theory and perfect SS indirect control approach are very useful to analyze which would be the best configuration of $\mathbf{G}_s(s)$ (Chang & Yu, 1990, 1992; Hori et al., 2005; Skogestad & Postlethwaite, 2005). From now on, the steady-state (SS) behavior ($s = 0$) is represented without the Laplace variable s.

Then, considering the IMC structure shown in Fig. 2, the optimal CVs selection can be made by considering the SS deviation of the UVs when perfect control ($\tilde{\mathbf{G}}_s = \mathbf{G}_s$) is assumed and both, set point and disturbance changes, are considered individually (Molina et al., 2011; Molina, Zumoffen, & Basualdo, 2009; Zumoffen & Basualdo, 2009), being, $\mathbf{G}_c = \tilde{\mathbf{G}}_s^{-1}$. Thus, at steady-state, the UVs of the process can be represented as

$$\mathbf{y}_r = \mathbf{G}_r\mathbf{G}_s^{-1}\mathbf{y}_s^{sp} + (\mathbf{D}_r - \mathbf{G}_r\mathbf{G}_s^{-1}\mathbf{D}_s)\mathbf{d}_* = \mathbf{S}_{sp}\mathbf{y}_s^{sp} + \mathbf{S}_d\mathbf{d}_* \quad (2)$$

with $\mathbf{y}_s^{sp}$ and $\mathbf{d}_*$ the set point and disturbance vectors and $\mathbf{S}_{sp} = \mathbf{G}_r\mathbf{G}_s^{-1}$ and $\mathbf{S}_d = (\mathbf{D}_r - \mathbf{G}_r\mathbf{G}_s^{-1}\mathbf{D}_s)$. From Eq. (2) it can be observed that

the UV deviations depend on the selected square subprocess $\mathbf{G}_s$ and if the set point and disturbance effects are considered individually, then, the SSD index can be stated as:

$$\begin{aligned}\text{SSD} &= \sum_{i=1}^{n} \|\Lambda_2 \mathbf{S}_{sp} \Lambda_1 \mathbf{y}_{sp}^n(i)\|_2^2 + \sum_{j=1}^{p} \|\Theta_2 \mathbf{S}_d \Theta_1 \mathbf{d}_*^p(j)\|_2^2 \\ &= \|\Lambda_2 \mathbf{S}_{sp} \Lambda_1\|_F^2 + \|\Theta_2 \mathbf{S}_d \Theta_1\|_F^2 \end{aligned} \tag{3}$$

where $\Lambda_2 \mathbf{S}_{sp} \Lambda_1 \mathbf{y}_{sp}^n(i)$ and $\Theta_2 \mathbf{S}_d \Theta_1 \mathbf{d}_*^p(j)$ are the vector of deviations corresponding to the $\mathbf{y}_r$ outputs from their nominal operating point values when an unitary change happens in the i set point and j disturbance respectively. The vectors $\mathbf{y}_{sp}^n(i)$ and $\mathbf{d}_*^p(j)$ have an unitary entry at the location i and j, and zero for the rest of the elements. The diagonal weighting matrices Λ_1 $(n \times n)$ and Θ_1 $(p \times p)$ allow to include the process control objectives such as set point/disturbance magnitudes (this is important when the used process model is not normalized), similarly, Λ_2 $((m-n) \times (m-n))$ and Θ_2 $((m-n) \times (m-n))$ take into account the relative degree of importance among the overall outputs. In addition, $\|\cdot\|_2$ represents the 2-norm for vectors and $\|\cdot\|_F$ means the Frobenius norm for matrices.

Using a suitable parametrization of $\mathbf{G}_s$ (and eventually $\mathbf{G}_r$, $\mathbf{D}_s$ and $\mathbf{D}_r$) the optimal CVs selection problem can be stated using Eq. (3) as

$$\min_{\mathbf{G}_s} (\text{SSD}), \quad \text{subjectto} \quad \det(\mathbf{G}_s) \neq 0 \tag{4}$$

this minimization is done by solving a combinatorial problem whose dimension is $m!/(n!\,(m-n)!)$. The proposed methodology selects n rows from $\mathbf{G}_{m \times n}$ to build $\mathbf{G}_s$ that minimizes the SSD index. The constraint, $\det(\mathbf{G}_s) \neq 0$, avoids the selection of unfeasible solutions when IMC strategy is applied. Depending on the problem size, the minimization given by Eq. (4) can be done by exhaustive search or by implementing some mixed-integer optimization routine (deterministic or stochastic). In some previous works of the authors (Molina et al., 2011; Zumoffen & Basualdo, 2010) the signal selection methodology was performed based on genetic algorithms (GA). This stochastic global search strategy represents a suitable alternative solution to solve combinatorial problems.

2.1.1. Properties of the SSD minimization

In this section some mathematical insights are given for analyzing how the matrix properties of the subprocess $\mathbf{G}_s$ evolve along the solutions given by optimization in (4). The conclusions stated here are verified graphically in Section 3 in the context of several dynamic simulations.

The main objective in the optimization problem stated in Eq. (4) is to find the best set of output variables such that achieve a multivariable gain minimization (at steady-state), i.e. minimum deviations on UVs. This gain reduction is performed on the transfer matrices $\mathbf{S}_{sp}$ (setpoint change effects) and $\mathbf{S}_d$ (disturbance change effects) simultaneously, i.e. deviations of $\mathbf{y}_r$ from its nominal operating point are minimized. It will be shown that the minimization of Eq. (4) also drives to good controllable conditions of the selected $\mathbf{G}_s$, i.e. well-conditioned subprocess. Several pioneering works (Garcia & Morari, 1985; Grosdidier et al., 1985; Skogestad & Postlethwaite, 2005; Skogetad & Morari, 1987) have been analyzed the effects of ill-conditioned process in control structure design. Note that the converse is not necessarily true; maximizing the minimum singular value of $\mathbf{G}_s$ does not necessarily guarantee minimum deviations on UVs, i.e. minimum SSD.

Considering that $\mathbf{S}_{sp} = \mathbf{G}_r \mathbf{G}_s^{-1}$ and the Frobenius norm definition for matrices, some inequalities such as those given in Eqs. (5) and (6), can be useful (Golub & Van Loan, 1996; Horn & Johnson, 1990; Skogestad & Postlethwaite, 2005; Zumoffen, Molina, Nieto, & Basualdo, 2011) for getting interesting conclusions about the methodology presented here.

$$\frac{\underline{\sigma}(\mathbf{G}_r)}{\underline{\sigma}(\mathbf{G}_s)} \leq \overline{\sigma}(\mathbf{G}_r \mathbf{G}_s^{-1}) \leq \|\mathbf{G}_r \mathbf{G}_s^{-1}\|_F \tag{5}$$

$$\frac{\overline{\sigma}(\mathbf{G}_r)}{\overline{\sigma}(\mathbf{G}_s)} \leq \overline{\sigma}(\mathbf{G}_r \mathbf{G}_s^{-1}) \leq \|\mathbf{G}_r \mathbf{G}_s^{-1}\|_F \tag{6}$$

where $\underline{\sigma}(\mathbf{A})$ and $\overline{\sigma}(\mathbf{A})$ are the minimum and maximum singular values of the matrix $\mathbf{A}$. These expressions show a clear link between the functional cost, $\|\mathbf{S}_{sp}\|_F$, and the matrix properties of both $\mathbf{G}_s$ and $\mathbf{G}_r$. Particularly, the conditions of the former are important because it is the selected subprocess to be controlled.

In this context, and considering the submatrices or interlacing property (Horn & Johnson, 1990) the following instances for Eq. (6) can be stated,

$$0 \leq \overline{\sigma}(\mathbf{G}_r)/\overline{\sigma}(\mathbf{G}_s) \leq 1 \quad \text{and} \quad 1 \leq \overline{\sigma}(\mathbf{G}_r)/\overline{\sigma}(\mathbf{G}_s) \leq \|\mathbf{G}_r \mathbf{G}_s^{-1}\|_F \tag{7}$$

for $n > m/2$ and $n < m/2$ cases respectively. These relationships show that the functional cost minimization almost has no effect on $\overline{\sigma}(\mathbf{G}_s)$. The inequality at the left of Eq. (7) can be seen that the ratio of the maximum singular values is perfectly bounded regardless the functional cost profile. The inequality at the right side shows that when the functional cost is minimized the relationship between $\overline{\sigma}(\mathbf{G}_s)$ and $\overline{\sigma}(\mathbf{G}_r)$ tends to one. In other words, $\overline{\sigma}(\mathbf{G}_s)$ is bounded and with minimal modifications, note that $\overline{\sigma}(\mathbf{G}) \geq \overline{\sigma}(\mathbf{G}_s)$ for any permutation. This means that the real impact of the minimization is performed on the ratio shown in Eq. (5). This is true because changes in $\underline{\sigma}(\mathbf{G}_s)$ have stronger impact in the functional cost than those in $\overline{\sigma}(\mathbf{G}_s)$.

Remark 1. Minimization of $\|\mathbf{S}_{sp}\|_F^2$ (when $m > n$) leads to select the best rows of $\mathbf{G}$ to construct $\mathbf{G}_s$ such that the steady-state multivariable gain of $\mathbf{G}_r \mathbf{G}_s^{-1}$ is minimized (minimum UVs deviations due to set point changes) and consequently the matrix conditioning of $\mathbf{G}_s$ tends to be improved by increasing its minimum singular value $\underline{\sigma}(\mathbf{G}_s)$.

The other term that contributes in the SSD minimization is $\|\Theta_2 \mathbf{S}_d \Theta_1\|_F^2$ placed in the right side of Eq. (3). For simplicity, the term $\|\mathbf{S}_d\|_F$ is analyzed only. Since $\mathbf{S}_d = [\mathbf{D}_r - \mathbf{G}_r \mathbf{G}_s^{-1} \mathbf{D}_s]$ and following an analogous reasoning as given before, the inequality Eq. (8) can be found (Golub & Van Loan, 1996; Horn & Johnson, 1990; Skogestad & Postlethwaite, 2005; Zumoffen et al., 2011).

$$|\overline{\sigma}(\mathbf{D}_r) - \overline{\sigma}(\mathbf{G}_r \mathbf{G}_s^{-1} \mathbf{D}_s)| \leq \overline{\sigma}(\mathbf{D}_r - \mathbf{G}_r \mathbf{G}_s^{-1} \mathbf{D}_s) \leq \|\mathbf{D}_r - \mathbf{G}_r \mathbf{G}_s^{-1} \mathbf{D}_s\|_F \tag{8}$$

again the submatrices property (Horn & Johnson, 1990; Skogestad & Postlethwaite, 2005) is fulfilled for the perturbation model $\max\{\overline{\sigma}(\mathbf{D}_r), \overline{\sigma}(\mathbf{D}_s)\} \leq \overline{\sigma}(\mathbf{D})$. Note that, if $\|\mathbf{D}_r - \mathbf{G}_r \mathbf{G}_s^{-1} \mathbf{D}_s\|_F \to 0$ then $\overline{\sigma}(\mathbf{G}_r \mathbf{G}_s^{-1} \mathbf{D}_s) \to \overline{\sigma}(\mathbf{D}_r)$. Using the singular value properties the following inequality can be stated,

$$\overline{\sigma}(\mathbf{G}_r \mathbf{G}_s^{-1} \mathbf{D}_s) \leq \overline{\sigma}(\mathbf{G}_r \mathbf{G}_s^{-1}) \overline{\sigma}(\mathbf{D}_s) \leq \frac{\overline{\sigma}(\mathbf{G}_r) \overline{\sigma}(\mathbf{D}_s)}{\underline{\sigma}(\mathbf{G}_s)} \tag{9}$$

the best scenario from the SSD minimization point of view is to have $\|\mathbf{D}_r - \mathbf{G}_r \mathbf{G}_s^{-1} \mathbf{D}_s\|_F = 0$, and in this case is obtained Eq. (10),

$$\underline{\sigma}(\mathbf{G}_s) \leq \frac{\overline{\sigma}(\mathbf{G}_r) \overline{\sigma}(\mathbf{D}_s)}{\overline{\sigma}(\mathbf{D}_r)} \tag{10}$$

The functional cost minimization affects $\underline{\sigma}(\mathbf{G}_s)$ because is the only source of singularity, i.e. the matrix properties of $\mathbf{G}_s$ are modified. But Eq. (10) shows that $\underline{\sigma}(\mathbf{G}_s)$ cannot be increased freely in this case. In fact, it is upper bounded by the process and disturbance transfer matrix characteristics.

Remark 2. Minimization of $\|\mathbf{S}_d\|_F^2$ (when $m > n$) leads to select the best rows of $\mathbf{G}$ to construct $\mathbf{G}_s$ such that the steady-state multivariable gain of $\mathbf{D}_r - \mathbf{G}_r \mathbf{G}_s^{-1} \mathbf{D}_s$ is minimized (minimum UVs deviations due to disturbances) and consequently the conditioning of $\mathbf{G}_s$ tends

to be improved by increasing its minimum singular value $\underline{\sigma}(\mathbf{G}_s)$. But in this case it is upper bounded by $\overline{\sigma}(\mathbf{G}_r)\overline{\sigma}(\mathbf{D}_s)/\overline{\sigma}(\mathbf{D}_r)$. Note that, a selection done based on min $\|\mathbf{S}_d\|_F^2$ could drive to a different solution than that obtained by min $\|\mathbf{S}_{sp}\|_F^2$.

The complemented and weighted functional cost stated in Eq. (3) was proposed for representing a trade-off solution between servo and regulator behaviors. If the weighting matrices Λ_1, Λ_2, Θ_1 and Θ_2 are used, then the partial control objective from synthesis stage, non normalized models and relative degree of importance between outputs can be accounted. The previous analysis is still valid in this case but now the new matrices become $\mathbf{S}_{sp}^* = \Lambda_2\mathbf{S}_{sp}\Lambda_1$ and $\mathbf{S}_d^* = \Theta_2\mathbf{S}_d\Theta_1$, and of course the new optimal solution may differ from the unweighted case.

It should be noted that the inequalities in Eqs. (5)–(10) were all tested numerically by several random matrices ($\mathbf{G}$ and $\mathbf{D}$) with different sizes (m, n, and p). This is a typical procedure for testing some developments as it is shown in Chang and Yu (1990), Grosdidier et al. (1985), and Kariwala and Cao (2010b) for example.

2.2. Controller structure design: defining the interaction level

Accounting Fig. 1 and assuming that the optimal CVs selection problem was solved efficiently (i.e. $\mathbf{G}_s(s)$ was selected), the problem to be addressed now is the input–output pairing, i.e. the controller structure design. The blocks with dark gray background in Fig. 1 allow to address this problem in a systematic and generalized way. Basically, this work is focussed on showing how the net load evaluation (NLE) approach allows to obtain the optimal control structure complementing the optimal CVs selection methodology. Note that the controller structure may be diagonal (i.e. decentralized/without interaction), full (i.e. centralized/full interaction) or sparse (i.e. partial interaction).

In this context, a good starting point is a decentralized control proposal as preliminary control structure (base case). Particularly in this work two input–output pairing approaches are suggested: the classical relative gain array (RGA) or its new version based on dynamic information the relative normalized gain array (RNGA) proposed by He et al. (2009). The RNGA was defined analogously to RGA as

$$\Lambda_N = \mathbf{K}_N \otimes (\mathbf{K}_N)^{-T}, \quad \text{with} \quad \mathbf{K}_N = \mathbf{G}_s \odot \mathbf{T} \tag{11}$$

where $\otimes$ is the element-by-element product, $\odot$ is the element-by-element division and $\mathbf{T}$ is a matrix containing information about the time constants and delay of each component in $\mathbf{G}_s(s)$. The RNGA effectively improves the pairing selection in some cases as it is shown in He et al. (2009) and Molina et al. (2011). Anyway, it is important to note that normalization proposed by $\mathbf{K}_N = \mathbf{G}_s \odot \mathbf{T}$ may produce some conditioning problems in $\mathbf{K}_N$, and obviously gives an erroneous pairing as is demonstrated in Zumoffen et al. (2011) for Petlyuk distillation column.

Thus, these issues must be considered into the MSD methodology. In fact, the RGA approach is preferred if any of the following conditions occur: (1) there is no available dynamic information, (2) the RGA and RNGA propose the same pairing or (3) $\mathbf{K}_N$ presents serious conditioning problems. In other cases, the RNGA is preferred.

Hence, the next step is to define the controller interaction level, i.e. analyze which kind of structures in the controller could improve the overall closed-loop response. In this work a controller structure design based on NLE is proposed. Chang and Yu (1992) have presented the generalized relative disturbance gain (GRDG) where the main concepts of net load effect first appear. GRDG method is a matrix approach (like RGA) to define classical control structures (diagonal, block diagonal, triangular, full) from disturbances rejection point of view. Here, this philosophy is extended/augmented including set point effects and proposing a new scalar index called net load evaluation (NLE) based on Frobenius norm. This augmented form allows us to deal with large-scale complex process in a generalized way avoiding matrix testing (very suitable for optimization routines). Moreover, the NLE strategy is augmented with a stability test based on IMC theory at steady-state. In fact, considering again Fig. 2, set points and disturbances, plant-model mismatch and IMC, the controlled outputs can be expressed in Laplace domain as,

$$\mathbf{y}_s(s) = \tilde{\mathbf{G}}_s(s)\mathbf{G}_c(s)\mathbf{y}_s^{sp}(s) + (\mathbf{I} - \tilde{\mathbf{G}}_s(s)\mathbf{G}_c(s))\mathbf{y}_s^{net}(s), \tag{12}$$

where

$$\mathbf{y}_s^{net}(s) = \mathbf{A}(s)\mathbf{y}_s^{sp}(s) + \mathbf{B}(s)\mathbf{d}_*(s) \tag{13}$$

$$\mathbf{A}(s) = [\mathbf{I} + (\mathbf{G}_s(s) - \tilde{\mathbf{G}}_s(s))\mathbf{G}_c(s)]^{-1}(\mathbf{G}_s(s) - \tilde{\mathbf{G}}_s(s))\mathbf{G}_c(s) \tag{14}$$

$$\mathbf{B}(s) = [\mathbf{I} + (\mathbf{G}_s(s) - \tilde{\mathbf{G}}(s))\mathbf{G}_c(s)]^{-1}\mathbf{D}_s(s), \tag{15}$$

with $\mathbf{B}(s)\mathbf{d}_*(s)$ the so called net load effect proposed for Chang and Yu (1992) and $\mathbf{y}_s^{net}(s)$ the augmented form proposed here accounting references and disturbances changes. Considering IMC design, $\mathbf{G}_c(s) = \tilde{\mathbf{G}}_s^{-1}(s)\mathbf{F}(s)$ and $\mathbf{F}(s)$ a diagonal low-pass TFM, the term $(\mathbf{I} - \tilde{\mathbf{G}}_s(s)\mathbf{G}_c(s))$ produces integral action rejecting the $\mathbf{y}_s^{net}(s)$ effects at steady-state in Eq. (12). Anyway, the real contribution of the net load is observed in the transient, when $(\mathbf{I} - \tilde{\mathbf{G}}_s(s)\mathbf{G}_c(s)) \approx \mathbf{I}$, and it is directly proportional to its multivariable gain. In fact, Eq. (12) can be written as

$$\mathbf{y}_s(s) = \mathbf{F}(s)\mathbf{y}_s^{sp}(s) + (\mathbf{I} - \mathbf{F}(s))\mathbf{y}_s^{net}(s), \tag{16}$$

from Eq. (16) two components are clearly identified in the right hand: (1) $\mathbf{F}(s)\mathbf{y}_s^{sp}(s)$ which is a filtered version of set point profiles, and (2) $(\mathbf{I} - \mathbf{F}(s))\mathbf{y}_s^{net}(s)$ a perturbation component involving the set point and disturbances changes. Obviously, the ideal situation is $\mathbf{y}_s(s) = \mathbf{F}(s)\mathbf{y}_s^{sp}(s)$ all the time. But, the second component effectively introduces undesired perturbations on $\mathbf{y}_s(s)$.

There are two scenarios for avoiding the $\mathbf{y}_s^{net}(s)$ effects,

1. Adjust the controller tuning, $\mathbf{F}$, for fast responses. This produces that all components in $(\mathbf{I} - \mathbf{F}(s))$ tends to zero as quickly as possible, and $\mathbf{y}_s^{net}(s)$ does not affect the CVs. But, it is a problematic solution since $\mathbf{F}$ cannot be adjusted freely due to stability issues, i.e. due to process dead times.
2. Minimize the multivariable gain of $\mathbf{y}_s^{net}(s)$, i.e. minimize both the $\mathbf{A}(s)\mathbf{y}_s^{sp}(s)$ and $\mathbf{B}(s)\mathbf{d}_*(s)$ effects simultaneously, according to Eq. (13). This can be done by minimizing $\mathbf{y}_s^{net}(s)$ at steady-state in a SSD sense. The tuning, in this case, is not modified.

In fact, the second approach presented above is selected here. Analyzing the structure of $\mathbf{y}_s^{net}(s)$ at steady-state ($\mathbf{F} = \mathbf{I}, \mathbf{G}_c = \tilde{\mathbf{G}}_s^{-1}$), Eqs. 14 and 15 can be expressed as:

$$\mathbf{A} = \mathbf{I} - \tilde{\mathbf{G}}_s\mathbf{G}_s^{-1} \tag{17}$$

$$\mathbf{B} = \tilde{\mathbf{G}}_s\mathbf{G}_s^{-1}\mathbf{D}_s \tag{18}$$

note that from Section 2.1 a well-conditioning in $\mathbf{G}_s$ is guaranteed, so there are no invertiability problems. Analyzing Eqs. (17) and (18) when $\tilde{\mathbf{G}}_s = \mathbf{G}_s$, i.e. a full IMC controller is used, then $\mathbf{A} = \mathbf{0}$ and $\mathbf{B} = \mathbf{D}_s$, so changes in the references do not affect $\mathbf{y}_s^{net}(s)$ (and therefore the CVs) but, in contrast, disturbances are not attenuated.

Remark 3. From Eqs. (12), (13), (17), and (18) it is observed that a specific plant-model mismatch, $\mathbf{G}_s - \tilde{\mathbf{G}}_s$, could produce both disturbance and reference changes attenuation from the $\mathbf{y}_s^{net}(s)$ point of view, and therefore minimize these effects on CVs (Eq. (16)). On the other hand, when a full IMC controller is used the best set point tracking is obtained ($\mathbf{A} = \mathbf{0}$). In practice, can occur that control structure design is determined as a trade-off between servo and regulator requirements.

The statements given in Note 3 do not agree with those presented by Shen et al. (2010). In fact, they conclude that some sparse control structures are the best choice for rejecting the interaction effects produced by set point changes. In the following sections it will be demonstrated that this is not true.

For minimizing the multivariable gain of $\mathbf{y}_s^{net}(s)$ a model parametrization for $\tilde{\mathbf{G}}_s$ it is required. In this context, the approach presented in Eq. (19) is suggested.

$$\tilde{\mathbf{G}}_{s\Gamma} = \mathbf{G}_s \otimes \Gamma, \quad \text{with} \quad \Gamma = \begin{bmatrix} \gamma_{11} & \cdots & \gamma_{1n} \\ \vdots & \ddots & \vdots \\ \gamma_{n1} & \cdots & \gamma_{nn} \end{bmatrix} \tag{19}$$

where γ_{ij} belongs to a binary alphabet $\{0,1\}$ indicating the selection ($\gamma_{ij}=1$) or not ($\gamma_{ij}=0$) of the ij process element. Using the parameterized model $\tilde{\mathbf{G}}_{s\Gamma}$ a new scalar index called net load evaluation (NLE) can be proposed in terms of a "sum square deviation" as it is shown in Eq. (20). The NLE index allows to both evaluate and decide about the best control structure (interaction level) that minimizes the multivariable gain of $\mathbf{y}_s^{net}$ at steady-state, i.e. minimize the deviations from their working point.

$$\begin{aligned} \mathrm{NLE}_\Gamma &= \sum_{i=1}^{n} \|\Delta_2 \mathbf{A}_\Gamma \Delta_1 \mathbf{y}_{sp}^n(i)\|_2^2 + \sum_{j=1}^{p} \|\Xi_2 \mathbf{B}_\Gamma \Xi_1 \mathbf{d}_*^p(j)\|_2^2 \\ &= \|\Delta_2 \mathbf{A}_\Gamma \Delta_1\|_F^2 + \|\Xi_2 \mathbf{B}_\Gamma \Xi_1\|_F^2 \end{aligned} \tag{20}$$

where Δ_1, Δ_2, Ξ_1 and Ξ_2 are diagonal weighting matrices which allow to sort the process control objectives according to its relative importance in the system, specially when the used process model is not normalized. The vectors $\mathbf{y}_{sp}^n(i)$ and $\mathbf{d}_*^p(j)$ have an unitary entry at the location i and j, and zero elsewhere. $\mathbf{A}_\Gamma$ and $\mathbf{B}_\Gamma$ are the net load matrices shown in Eqs. (17) and (18) parameterized with the model selection displayed in Eq. (19). Hence, the combinatorial problem shown in Eqs. (21) and (22) allows to find the optimal model parametrization and gives a good guide for the control structure selection via IMC.

$$\min_\Gamma \mathrm{NLE}_\Gamma = \min_\Gamma \left[\|\Delta_2 \mathbf{A}_\Gamma \Delta_1\|_F^2 + \|\Xi_2 \mathbf{B}_\Gamma \Xi_1\|_F^2 \right] \tag{21}$$

subject to

$$\mathrm{Re}[\lambda_i(\mathbf{G}_s \tilde{\mathbf{G}}_{s\Gamma}^{-1})] > 0, \quad \text{with} \quad i = 1, \ldots, n \tag{22}$$

where $\mathrm{Re}[\cdot]$ is the real part function, $\lambda_i(\cdot)$ is the ith eigenvalue, and $\tilde{\mathbf{G}}_{s\Gamma}$ the model parametrization/selection. Inequality in Eq. (22) is the stability/robustness criterion developed by Garcia and Morari (1985) for multivariable control structures based on IMC theory. The optimization problem in Eq. (21) has $2^{(n\times n)}$ potential solutions. According to the problem size, this minimization can be done by exhaustive search or implementing some mixed-integer optimization routine (deterministic or stochastic). In some previous works of the authors (Molina et al., 2011; Zumoffen & Basualdo, 2010) good solutions were found applying genetic algorithms (GA).

2.2.1. Decentralized structure as starting point

The MSD approach suggests an initial input–output pairing based on RGA or RNGA. So, the basic idea here is considering this decentralized control structure as starting point in the combinatorial problem defined in Eq. (21). In other words, keep the diagonal pairing as base case structure in the parametrization matrix displayed in Eq. (19) and evaluate only the off-diagonal elements required to minimize de NLE. Thus, $\mathbf{G}_s$ must be configured as diagonal input–output pairing (i.e. row or column reordering) before the evaluation. The parametrization matrix suggested in Eq. (19) results in this case

$$\begin{aligned} \Gamma &= \begin{bmatrix} 1 & \gamma_{12} & \cdots & \gamma_{1n} \\ \gamma_{21} & 1 & \cdots & \gamma_{2n} \\ \vdots & \vdots & \ddots & \vdots \\ \gamma_{n1} & \cdots & \cdots & 1 \end{bmatrix} = \begin{bmatrix} 1 & 0 & \cdots & 0 \\ 0 & 1 & \cdots & 0 \\ \vdots & \vdots & \ddots & \vdots \\ 0 & \cdots & \cdots & 1 \end{bmatrix} \\ &+ \begin{bmatrix} 0 & \gamma_{12} & \cdots & \gamma_{1n} \\ \gamma_{21} & 0 & \cdots & \gamma_{2n} \\ \vdots & \vdots & \ddots & \vdots \\ \gamma_{n1} & \cdots & \cdots & 0 \end{bmatrix} = \Gamma_d + \Gamma_{od} \end{aligned} \tag{23}$$

where $\Gamma_d = \mathbf{I}_n$ represents the diagonal pairing (via RGA or RNGA) and Γ_{od} gives the off-diagonal parametrization matrix where the searching is effectively performed. In this context the problem dimension is reduced to $2^{(n\times n-n)}$. Thus, the Hadamard product in Eq. 19 can be expressed as:

$$\tilde{\mathbf{G}}_{s\Gamma} = \mathbf{G}_s \otimes \Gamma = \mathbf{G}_s \otimes \Gamma_d + \mathbf{G}_s \otimes \Gamma_{od} = \tilde{\mathbf{G}}_{s\Gamma_d} + \tilde{\mathbf{G}}_{s\Gamma_{od}} \tag{24}$$

where $\tilde{\mathbf{G}}_{s\Gamma_d}$ and $\tilde{\mathbf{G}}_{s\Gamma_{od}}$ are the process model approximations by accounting a decentralized/diagonal structure and an off-diagonal parametrization respectively. The net load matrices in Eqs. (17) and (18) become

$$\mathbf{A}_\Gamma = \mathbf{I} - \tilde{\mathbf{G}}_{s\Gamma} \mathbf{G}_s^{-1} = \mathbf{I} - (\tilde{\mathbf{G}}_{s\Gamma_d} + \tilde{\mathbf{G}}_{s\Gamma_{od}}) \mathbf{G}_s^{-1} = (\mathbf{I} - \tilde{\mathbf{G}}_{s\Gamma_d} \mathbf{G}_s^{-1}) - \tilde{\mathbf{G}}_{s\Gamma_{od}} \mathbf{G}_s^{-1} \tag{25}$$

$$\mathbf{B}_\Gamma = \tilde{\mathbf{G}}_{s\Gamma} \mathbf{G}_s^{-1} \mathbf{D}_s = (\tilde{\mathbf{G}}_{s\Gamma_d} + \tilde{\mathbf{G}}_{s\Gamma_{od}}) \mathbf{G}_s^{-1} \mathbf{D}_s = \tilde{\mathbf{G}}_{s\Gamma_d} \mathbf{G}_s^{-1} \mathbf{D}_s + \tilde{\mathbf{G}}_{s\Gamma_{od}} \mathbf{G}_s^{-1} \mathbf{D}_s \tag{26}$$

note that $(\mathbf{I} - \tilde{\mathbf{G}}_{s\Gamma_d} \mathbf{G}_s^{-1})$ and $\tilde{\mathbf{G}}_{s\Gamma_d} \mathbf{G}_s^{-1} \mathbf{D}_s$ are fixed, i.e. depend on the process matrices and the diagonal pairing selected, Γ_d. In contrast, components $-\tilde{\mathbf{G}}_{s\Gamma_{od}} \mathbf{G}_s^{-1}$ and $\tilde{\mathbf{G}}_{s\Gamma_{od}} \mathbf{G}_s^{-1} \mathbf{D}_s$ are parameterized as function of Γ_{od}, i.e. where the searching is effectively performed. Thus, the NLE approach defines the best controller interaction level by selecting (or not) specific off-diagonal elements in the process model, considering the decentralized structure as base case.

Note that, Eqs. (25) and (26) define the optimization problem stated in Eq. (21), but the stability condition in Eq. (22) is evaluated by accounting the complete parametrization, $\tilde{\mathbf{G}}_{s\Gamma}$, i.e. the overall plant-model mismatch.

2.3. Controller tuning

Considering the TFM of the square process factorized as $\tilde{\mathbf{G}}_{s\Gamma}(s) = \tilde{\mathbf{G}}_{s\Gamma}^-(s)\tilde{\mathbf{G}}_s^+(s)$ (Garcia & Morari, 1985), with $\tilde{\mathbf{G}}_{s\Gamma}^-(s)$ and $\tilde{\mathbf{G}}_s^+(s)$ are the invertible and non invertible parts respectively. Then a practical IMC implementation suggests the following controller to the Fig. 2, $\mathbf{G}_c(s) = \tilde{\mathbf{G}}_{s\Gamma}^-(s)^{-1}\mathbf{F}(s)$. Where $\mathbf{F}(s) = \mathrm{diag}([1/(\tau_{f1}s+1)\ldots 1/(\tau_{fn}s+1)])$ is the low-pass filter TFM for robustness to modeling errors purposes. In this work an IMC design based on models without delay information are used, i.e. $\tilde{\mathbf{G}}_s^+(s) = \mathbf{I}$. Filter time constant, τ_{fi}, affect the ith input channel of the process and due to $\tilde{\mathbf{G}}_{s\Gamma}$ fulfills with Eq. (22) a preliminary and conservative tuning is proposed such as: $\tau_{fi} \geq \max_j(\theta_{ji})$, with $j = 1, \ldots, n$.

2.4. Summary of the MSD approach

Considering the developments made in previous sections, the layout displayed in Fig. 1, and a process already stabilized the following basic steps can be defined for the MSD approach:

1. Define the potential CVs and MVs and evaluate its steady-state gain (or dynamic model if it is feasible).
2. Evaluate the degrees of freedom (DF). If there are no DF go to step no. 4.
3. Select the optimal CVs via SSD minimization in Eqs. (3) and (4), i.e. define $\mathbf{G}_s$. Incorporate here any a priori control objectives by using the weighting matrices.
4. Perform the input–output pairing via RGA or RNGA, i.e. a decentralized control structure is defined.
5. Analyze the potential improvements via NLE minimization (sparse control) from Eqs. (20)–(22). Use the parametrization given in Eq. (23). Incorporate here any a priori control objectives by using the weighting matrices.
6. Compare dynamically the obtained control structures and perform a robust stability test.
7. Select the control structure with the minimum SSD and NLE index and lowest μ peak value.

The weighting matrices in Eq. (3) allow including some a priori information in the CVs selection procedure such as locations, magnitudes, important variables, etc. Indeed, Λ_1 and Θ_1 have information about the usual/required reference and disturbance modifications. Moreover, not normalized models can be considered into the MSD approach by setting these matrices with nominal percentage modifications. For example, all the variables which are required to modify its operating point (partial control requisites from Process Engineering) will be CV indefectibly. Hence, these variables will be fixed into the $\mathbf{G}_s$ and they will have reference changes in Λ_1. On the other hand, matrices Λ_2 and Θ_2 have information about the relative degree of importance among the uncontrolled outputs. In fact, these matrices allow defining if all the UVs are equally weighted or any specific UV (or group of them) is weighted particularly. The latter is useful for indirect control purposes. The entries values for these matrices are related to the process model, i.e. if the model is normalized or not.

3. Simulation results

In this section several case studies are presented. The procedures stated in Sections 2.1 and 2.2 are used here to develop plant-wide control structures. Initially, the case studies are divided in two classes: square and non-square process, because they require different treatments. In fact, both the optimal CVs selection and controller structure design approaches can be applied to the latter and only the controller design methodology can be tested in the former cases. The controller tuning is shown in Appendix A. Finally, the overall process layout and the selected control structure for each case study are shown in Appendix B.

3.1. Non-square processes

3.1.1. Shell oil fractionator

The Shell oil fractionator process presented in Maciejowski (2002) is considered here. The stabilized plant has 7 potential CVs, 3 MVs, and 2 DVs. The first order plus delay (FOPD) transfer functions are displayed in Table 1, with **Outputs:** y_1 and y_2 top and side end point compositions, y_3 to y_7 top, upper reflux, side draw, intermediate reflux and bottom temperatures, **Inputs:** u_1 and u_2 top and side draw flows, u_3 bottoms reflux duty, **Disturbances:** d_1 and d_2 intermediate and upper reflux duty (see Appendix B, Fig. 10(a)).

In this context, the optimal CVs selection approach based on SSD is applied with $m=7$, $n=3$, $p=2$, $\Lambda_1=\mathbf{I}_3$, $\Lambda_2=\mathbf{I}_4$, $\Theta_1=\mathbf{I}_2$, and $\Theta_2=\mathbf{I}_4$, where $\mathbf{I}_i$ is the identity matrix of $i\times i$. A combinatorial problem with $7!/(3!(7-3)!)=35$ potential solutions can be stated according to Eq. (4), so an exhaustive search is feasible. Fig. 3 summarizes the most important matrix properties involved in the SSD minimization. The profiles of both functional cost and condition number of $\mathbf{G}_s$ are shown in Fig. 3(a) with logarithmic scale (y-axes). On the other hand, Fig. 3(b) displays the minimum and maximum singular values of $\mathbf{G}_s$ along the solutions. Note that for both figures the solutions have been sorted from the best (left) to the worst (right). It is clear that the optimal solution represents a well conditioned $\mathbf{G}_s$ which minimizes both the multivariable gain SSD and the condition number.

Table 1
Shell oil fractionator model.

	$\mathbf{G}(s)$			$\mathbf{D}(s)$	
	u_1	u_2	u_3	d_1	d_2
y_1	$\frac{4.05e^{-27s}}{50s+1}$	$\frac{1.77e^{-28s}}{60s+1}$	$\frac{5.88e^{-27s}}{50s+1}$	$\frac{1.20e^{-27s}}{45s+1}$	$\frac{1.44e^{-27s}}{40s+1}$
y_2	$\frac{5.39e^{-18s}}{50s+1}$	$\frac{5.72e^{-14s}}{60s+1}$	$\frac{6.90e^{-15s}}{40s+1}$	$\frac{1.52e^{-15s}}{25s+1}$	$\frac{1.83e^{-15s}}{20s+1}$
y_3	$\frac{3.66e^{-2s}}{9s+1}$	$\frac{1.65e^{-20s}}{30s+1}$	$\frac{5.53e^{-2s}}{40s+1}$	$\frac{1.16}{11s+1}$	$\frac{1.27}{6s+1}$
y_4	$\frac{5.92e^{-11s}}{12s+1}$	$\frac{2.54e^{-12s}}{27s+1}$	$\frac{8.10e^{-2s}}{20s+1}$	$\frac{1.73}{5s+1}$	$\frac{1.79}{19s+1}$
y_5	$\frac{4.13e^{-5s}}{8s+1}$	$\frac{2.38e^{-7s}}{19s+1}$	$\frac{6.23e^{-2s}}{10s+1}$	$\frac{1.31}{2s+1}$	$\frac{1.26}{22s+1}$
y_6	$\frac{4.06e^{-8s}}{13s+1}$	$\frac{4.18e^{-4s}}{33s+1}$	$\frac{6.53e^{-s}}{9s+1}$	$\frac{1.19}{19s+1}$	$\frac{1.17}{24s+1}$
y_7	$\frac{4.38e^{-20s}}{33s+1}$	$\frac{4.42e^{-22s}}{44s+1}$	$\frac{7.20}{19s+1}$	$\frac{1.14}{27s+1}$	$\frac{1.26}{32s+1}$

The best first five solutions given by the search are shown in Table 2 with their corresponding SSD indexes. Note that, s_i has a direct correspondence to y_i in Table 1, with $i=1,\ldots,7$. The optimal solution, S_1, selects y_2, y_4 and y_7 as the best CVs selection. But accounting the original control requisites stated by Maciejowski (2002), it is important to ensure the products quality (y_1 and y_2). Hence, the best solution to this problem is, S_3, which selects y_1 (top composition), y_2 (side composition) and y_7 (bottom temperature), marked with (*) in the table. Thus, both the control requisites and the SSD minimization are fulfilled. Note that Λ_2 and Θ_2 were adjusted to perform a free searching, i.e. the same relative degree of importance among variables.

Following the MSD procedure (Fig. 1), the next step is a RGA and RNGA testing. Considering Section 2.2 and the process model in Table 1 both approaches suggest the same input–output pairing: u_1-y_1, u_2-y_2 and u_3-y_7 as a preliminary decentralized control strategy. Anyway, it is important to note that RGA is computed using $\mathbf{G}_s$ where $\det(\mathbf{G}_s)=20.8$ and $\underline{\sigma}(\mathbf{G}_s)=0.6$ and the RNGA approach on $\mathbf{K}_N$ with $\det(\mathbf{K}_N)=6.2\times10^{-4}$ and $\underline{\sigma}(\mathbf{K}_N)=0.02$. It is a clear example of how the RNGA normalization can deteriorate the matrix properties. In this context, the following evaluation is the NLE approach via Eq. (21) with the parametrization suggested in Section 2.2.1, thus the combinatorial problem has $2^{(3\times3-3)}=64$ potential solutions and can be evaluated exhaustively. In this case two set of weighting matrices are proposed: (1) equally weighting

Table 2
Best first five solutions - Shell process.

	CVs Selected							
S_i	s_1	s_2	s_3	s_4	s_5	s_6	s_7	SSD
1	0	1	0	1	0	0	1	2.37
2	0	1	0	1	0	1	0	3.26
3*	1	1	0	0	0	0	1	4.83
4	1	1	0	0	0	1	0	5.59
5	0	1	1	0	0	0	1	6.68

The gray background represents the selection suggested.

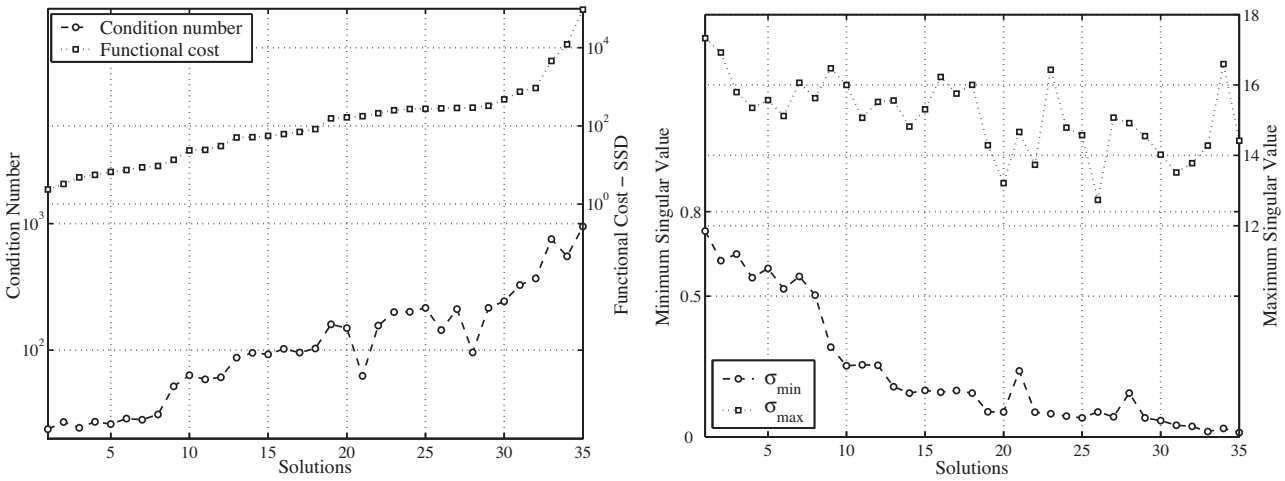

(a) Condition number and functional cost (b) Maximum and minimum singular values

Fig. 3. Optimal CVs selection via SSD – Shell process. (a) Condition number and functional cost. (b) Maximum and minimum singular values.

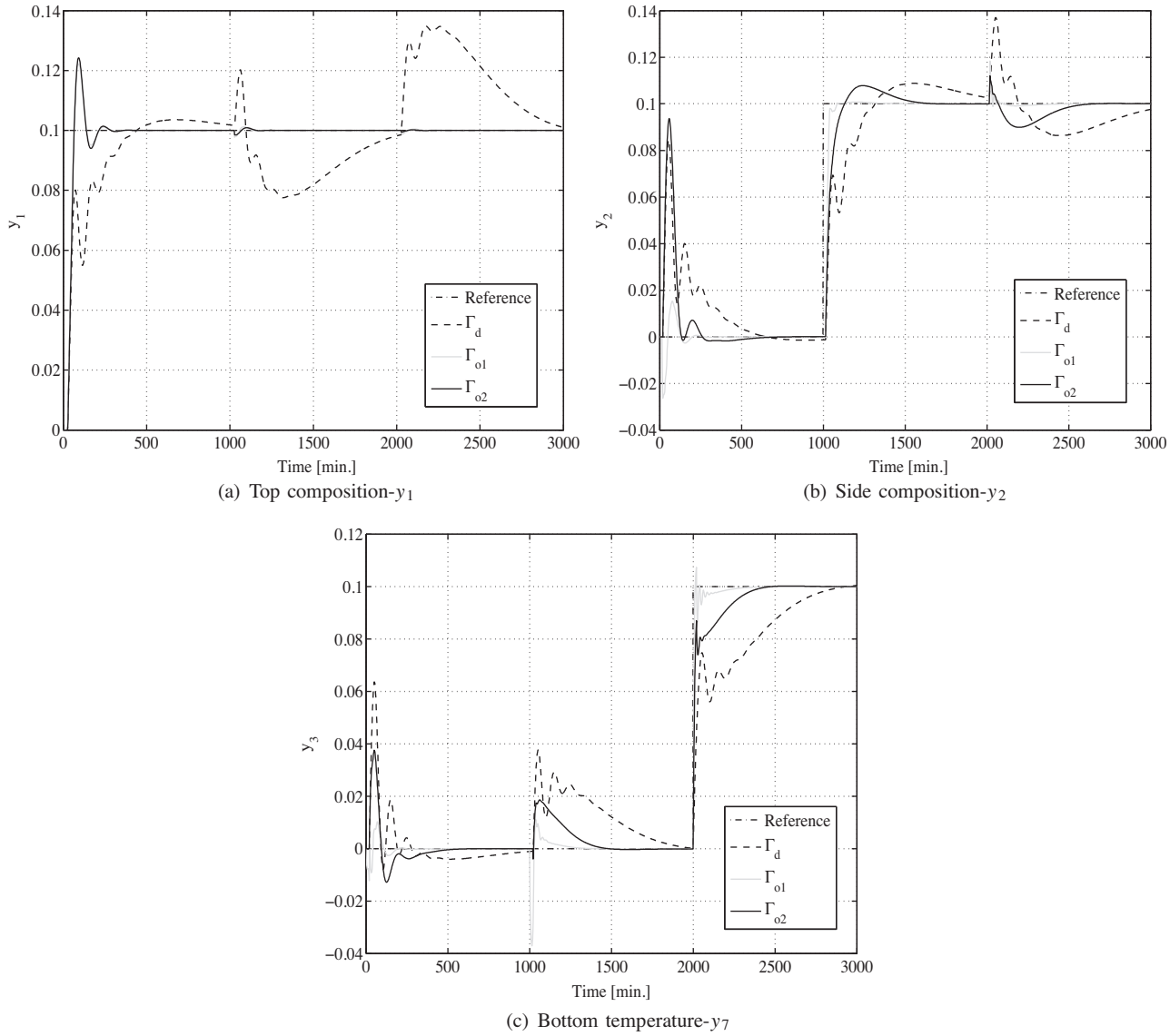

(a) Top composition-y_1 (b) Side composition-y_2

(c) Bottom temperature-y_7

Fig. 4. Shell process – Servo profiles. (a) Top composition-y_1; (b) side composition-y_2; and (c) bottom temperature-y_7.

Table 3
Shell process – IAE indexes.

Γ	Servo	Regulator
Γ_{o1}	14.06	23.78
Γ_{o2}	33.20	36.35
Γ_d	111.20	50.83

The best performances are highlighted with gray background.

with $\Delta_1 = \mathbf{I}_3 0.5$, $\Delta_2 = \mathbf{I}_3$, $\Xi_1 = \mathbf{I}_2 0.5$ and $\Xi_2 = \mathbf{I}_3$, and (2) reference relaxed weighting with $\Delta_1 = \mathbf{I}_3 0.1$, $\Delta_2 = \mathbf{I}_3$, $\Xi_1 = \mathbf{I}_2 0.5$ and $\Xi_2 = \mathbf{I}_3$. Obviously, these settings give different model selections and controller structures called Γ_{o1} and Γ_{o2} respectively. These proposals are shown in Eq. (27), and compared via dynamic simulations in Fig. 4.

$$\Gamma_d = \begin{bmatrix} 1 & 0 & 0 \\ 0 & 1 & 0 \\ 0 & 0 & 1 \end{bmatrix}, \quad \Gamma_{o1} = \begin{bmatrix} 1 & 1 & 1 \\ 1 & 1 & 1 \\ 1 & 1 & 1 \end{bmatrix}, \quad \Gamma_{o2} = \begin{bmatrix} 1 & 1 & 1 \\ 0 & 1 & 0 \\ 0 & 0 & 1 \end{bmatrix} \tag{27}$$

Fig. 4 summarizes the servo behavior of the process when the controller structures suggested by Eq. (27) are implemented on the Shell plant. In this case, step changes (0.1) are proposed sequentially at $t = 0$, $t = 1000$, and $t = 2000$ min for all set points. Clearly, decentralized control based on Γ_d presents the worst behavior. On the other hand and consistent with conclusion stated in Section 2.2 (Note 3) the best servo performance corresponds to the full structure, Γ_{o1}, and the second optimal one based on Γ_{o2} displays an intermediate behavior between decentralized and full approaches. Moreover, in Table 3 the total IAE (sum of IAE for each output) between outputs and references are presented for servo and regulator scenarios. The latter is computed by considering sequential disturbances in $d_1 = 0.1$ and $d_2 = 0.1$ at $t = 100$ and $t = 1100$ min respectively with a total simulation time of 2100 min.

In this case, an interacting control structure may be the best choice. From Table 3 controllers based on Γ_{o1} or Γ_{o2} have improvements respect to the decentralized one about "≈87.3% and ≈53.2%", and "≈70.2% and ≈28.5%" respectively when servo and regulator scenarios are considered.

3.1.2. Newell and Lee evaporator

In this case the Newell and Lee evaporator is used as a non-square control problem. The process is presented as a non-linear model and described in detail by Maciejowski (2002) and Govatsmark and Skogestad (2001). Here, the plant-wide control problem is considered with: **Outputs:** y_1 product composition, y_2 operating pressure, y_3 product temperature, y_4 vapor separator temperature, y_5 vapor separator flow rate, y_6 steam jacket duty, y_7 evaporator steam flow rate, and y_8 separator level, **Inputs:** u_1 steam pressure, u_2 cooling water flow rate, u_3 circulating flow rate, and u_4 product flow rate, **Disturbances:** d_1 feed flow rate, d_2 feed concentration, d_3 feed temperature, and d_4 cooling water entry temperature (see Appendix B, Fig. 10(b)).

The process is open-loop unstable due to y_8. Early works (Govatsmark & Skogestad, 2001; Maciejowski, 2002) suggest u_4 as the best selection to stabilize the plant. Moreover, u_3 is not used as MV (Govatsmark & Skogestad, 2001). Thus, the overall control problem becomes to 7 CVs (y_1 to y_7), 2 MVs (u_1 and u_2) and 4 DVs (d_1 to d_4).

After stabilizing the plant and before the optimal CVs selection application, a simplified model of the non-linear process is required. In this work a system identification (SI) experiment is used based on sub-space methods (Ljung, 1999). In this case a discrete linear model of eighth order was obtained, with a sample time of 2 min, and based on historical (normalized) data.

With a simplified model already available the next step is the optimal CVs selection approach via SSD minimization with $m = 7$, $n = 2$ and $p = 4$, which represents a combinatorial problem with $7!/(2!(7-2)!) = 21$ potential solutions and an exhaustive search is feasible. To solve Eq. (4) in this case $\Lambda_1 = \mathbf{I}_2$, $\Lambda_2 = \mathbf{I}_5$, $\Theta_1 = \mathbf{I}_4$, and $\Theta_2 = \mathbf{I}_5$ is used. Fig. (5) summarizes the most important matrix properties involved in the SSD minimization. The profiles of both functional cost and condition number of $\mathbf{G}_s$ are shown in Fig. (5)(a) with logarithmic scale (y-axes). On the other hand, Fig. 5(b) displays the minimum and maximum singular values of $\mathbf{G}_s$ along the solutions. Note that for both figures the solutions have been sorted from the best (left) to the worst (right). It is clear that the optimal solution represents a well conditioned $\mathbf{G}_s$ which minimizes both the multivariable gain SSD and the condition number.

The best first five solutions and the SSD indexes given by the search are shown in Table 4. Note that, s_i has a direct correspondence to y_i, with $i = 1, \ldots, 7$. The first two solutions, S_1 and S_2, have virtually the same SSD index, but the former suggests y_1 and y_4 as CVs, and the latter y_1 and y_2. A priori these two solutions are equally valid, but for safety it is preferable to control the operating

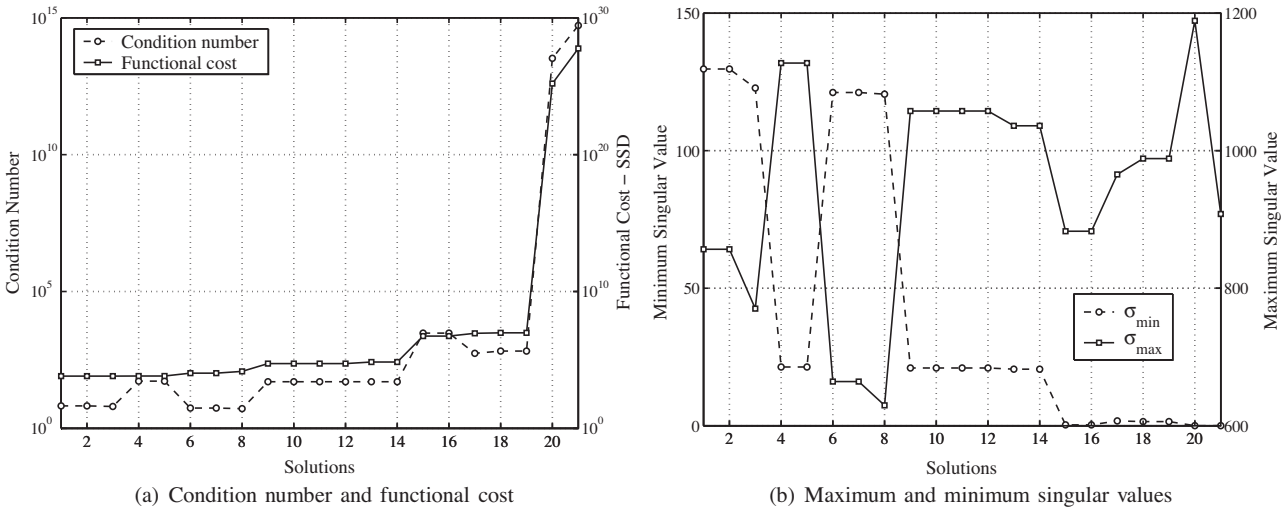

(a) Condition number and functional cost (b) Maximum and minimum singular values

Fig. 5. Optimal CVs selection via SSD – Evaporator process. (a) Condition number and functional cost and (b) maximum and minimum singular values.

Table 4
Best first five solutions - Evaporator process.

	MVs Selected							
S_i	s_1	s_2	s_3	s_4	s_5	s_6	s_7	SSD
1	1	0	0	1	0	0	0	6566.7
2*	1	1	0	0	0	0	0	6566.7
3	1	0	1	0	0	0	0	6568.3
4	0	1	1	0	0	0	0	6603.6
5	0	0	1	1	0	0	0	6603.6

The gray background represents the selection suggested.

pressure (y_2) instead of vapor separator temperature (y_4). Hence, the best solution to this problem is S_2 marked with (*) in Table 4. It is important to comment that the process, $\mathbf{G}_s(s)$, suggested by both solutions (S_1 and S_2) were controlled with a decentralized structure and both showed the same good dynamic performance.

The RGA and RNGA suggest the same input–output pairing: $u_1 - y_1$ and $u_2 - y_2$ as a preliminary decentralized control strategy. Again, for this example it can be detected that the RNGA normalization deteriorates the matrix properties. In this context, the following evaluation is the NLE approach via Eq. (21) with the parametrization suggested in Section 2.2.1, thus the combinatorial problem has $2^{(2\times2-2)} = 4$ potential solutions and can be evaluated exhaustively. In this case an equally weighting is suggested with $\Delta_1 = \mathbf{I}_2$, $\Delta_2 = \mathbf{I}_2$, $\Xi_1 = \mathbf{I}_4$ and $\Xi_2 = \mathbf{I}_2$. The optimal solution is called Γ_{o1} and represents a full parametrization as is shown in Eq. (28). Moreover, two alternative model selections are displayed: Γ_d for a decentralized control structure and Γ_{o2} which is the second best solution in the combinatorial problem and represents a sparse controller structure. All these proposals are compared via non-linear dynamic simulations in Fig. 6.

$$\Gamma_d = \begin{bmatrix} 1 & 0 \\ 0 & 1 \end{bmatrix}, \quad \Gamma_{o1} = \begin{bmatrix} 1 & 1 \\ 1 & 1 \end{bmatrix}, \quad \Gamma_{o2} = \begin{bmatrix} 1 & 0 \\ 1 & 1 \end{bmatrix} \tag{28}$$

Fig. 6 summarizes the process servo behavior when the controller structures suggested by the model selection displayed in Eq. (28) are implemented on the non-linear evaporator. In this case,

Table 5
Evaporator process – IAE indexes.

Γ	Servo	Regulator
Γ_{o1}	61.08	116.55
Γ_{o2}	91.51	109.56
Γ_d	96.93	119.46

The best performances are highlighted with gray background.

step changes of +5% respect to the operating point are proposed sequentially at $t = 200$, $t = 600$ min for all references. Clearly the full control structure Γ_{o1}, presents the best servo performance which reinforces the statements given in Section 2.2 (Note 3). On the other hand, decentralized and sparse control Γ_d and Γ_{o2} respectively display a similar servo behavior. Moreover, in Table 5 the total IAE (sum of IAE for each output) between outputs and references are presented for servo and regulator scenarios. The latter is computed by considering sequential disturbances in $d_1 = d_2 = d_3 = d_4 = +5\,\%$ at $t = 200$, 600, 1000, and 1400 min respectively with a total simulation time of 1800 min. In this case, an interacting control structure, either based on Γ_{o1} or Γ_{o2}, is preferred because both have improvements respect to the decentralized case of about "≈37% and ≈2.5%", and "≈6% and ≈8.3%" respectively when servo and regulator scenarios are considered.

3.2. Square processes

In this section the basic idea is showing the MSD procedure on already square process control problems. In fact, the subroutine called control structure design via NLE minimization can be applied in these cases to evaluate several alternative controller structures.

3.2.1. Ogunnaike and Ray process

The Ogunnaike and Ray (OR) process (Luyben, 1986; Monica et al., 1988) is a well-known distillation column for ethanol-water separation. The open-loop reduced model is shown in Table 6 and represents a 3×3 square process. Where y_1 and y_2 are the top and side compositions respectively, y_3 the tray 19 temperature, u_1 the top reflux, u_2 the side flow, u_3 is the reboiler pressure and d_1 represents disturbances in the feed flow (see Appendix B, Fig. 10(c)).

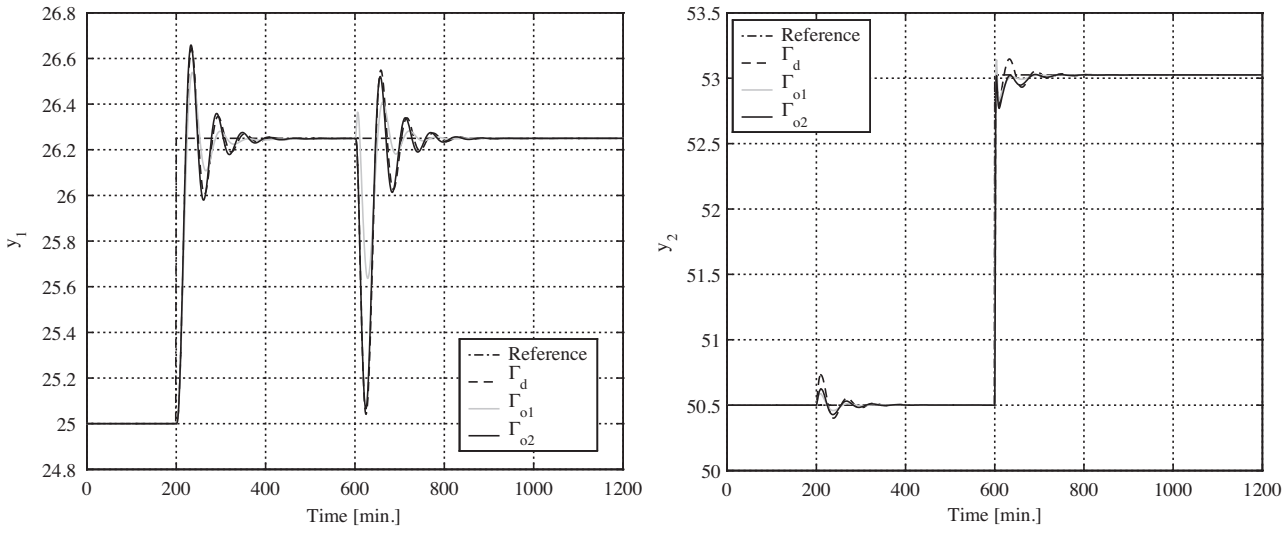

(a) Product composition-y_1 (b) Operating pressure-y_2

Fig. 6. Evaporator process – Servo profiles. (a) Product composition – y_1; and (b) operating pressure – y_2.

Table 6
OR process model.

	$\mathbf{G}_s(s)$			$\mathbf{D}_s(s)$
	u_1	u_2	u_3	d_1
y_1	$\frac{0.66e^{-2.6s}}{(6.7s+1)}$	$\frac{-0.61e^{-3.5s}}{(8.64s+1)}$	$\frac{-0.0049e^{-s}}{(9.06s+1)}$	$\frac{0.14e^{-12s}}{(19.2s+1)^2}$
y_2	$\frac{1.11e^{-6.5s}}{(3.25s+1)}$	$\frac{-2.36e^{-3s}}{(5s+1)}$	$\frac{-0.01e^{-1.2s}}{(7.09s+1)}$	$\frac{0.53e^{-10.5s}}{(6.9s+1)}$
y_3	$\frac{-34.68e^{-9.2s}}{(8.15s+1)}$	$\frac{46.2e^{-9.4s}}{(10.9s+1)}$	$\frac{0.87(11.61s+1)e^{-s}}{(3.89s+1)(18.8s+1)}$	$\frac{-11.54e^{-0.6s}}{(7.01s+1)}$

Accounting the MSD procedure in Fig. 1 and Section 2.2, the RGA and RNGA testing suggest the same input–output pairing: $u_1 - y_1$, $u_2 - y_2$, and $u_3 - y_3$ as a preliminary decentralized control strategy. The following evaluation is the NLE approach via Eq. (21) with the parametrization suggested in Section 2.2.1, thus the combinatorial problem to be solved has $3^{(3\times3-3)} = 64$ potential solutions and can be evaluated exhaustively. In this case an equally weighting: $\Delta_1 = \mathbf{I}_3$, $\Delta_2 = \mathbf{I}_3$, $\Xi_1 = 1$ and $\Xi_2 = \mathbf{I}_3$, and reference relaxed weighting: $\Delta_1 = \mathbf{I}_3 0.2$, $\Delta_2 = \mathbf{I}_3$, $\Xi_1 = 1$ and $\Xi_2 = \mathbf{I}_3$ scenarios are proposed. These settings generate the Γ_{o1} and Γ_{o2} optimal solutions for model selection respectively, as it is shown in Eq. (29). Clearly, both parameterizations give a full and a sparse control structures respectively. Moreover, two alternative model selections are suggested for comparison purposes: Γ_{dS} and Γ_{oS} which represent the decentralized and sparse no.1 control structures proposed by Shen et al. (2010) based on the equivalent transfer function approach. All these proposals are compared via dynamic simulations in Fig. 7.

$$\Gamma_{o1} = \begin{bmatrix} 1 & 1 & 1 \\ 1 & 1 & 1 \\ 1 & 1 & 1 \end{bmatrix} \Gamma_{o2} = \begin{bmatrix} 1 & 1 & 1 \\ 1 & 1 & 0 \\ 0 & 0 & 1 \end{bmatrix} \Gamma_{dS} = \begin{bmatrix} 1 & 0 & 0 \\ 0 & 1 & 0 \\ 0 & 0 & 1 \end{bmatrix} \Gamma_{oS} = \begin{bmatrix} 1 & 1 & 0 \\ 1 & 1 & 0 \\ 0 & 0 & 1 \end{bmatrix} \tag{29}$$

Fig. 7 displays the regulator profiles of the closed-loop process when the controller structure suggested by the model selections shown in Eq. (29) are implemented. In this case, a unit step change at $t = 100$ s. is proposed for the disturbance. Clearly, the full Γ_{o1} and decentralized Γ_{dS} based controller design present the best performance. Moreover, accounting Table 7, the total IAE for the servo scenario can be evaluated also. In fact, again the statement given in

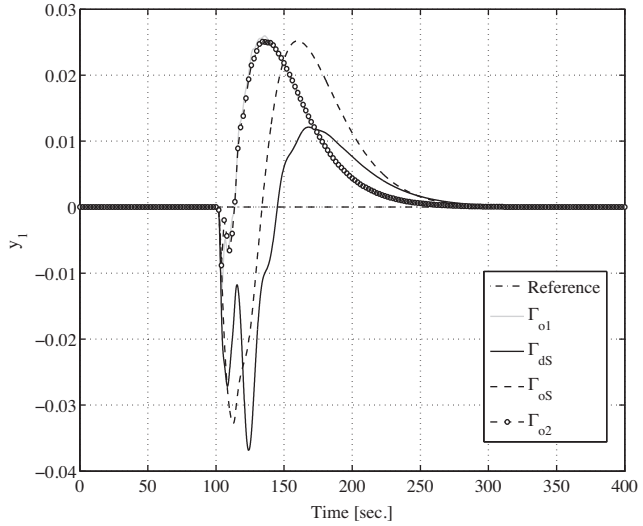

(a) Top composition-y_1

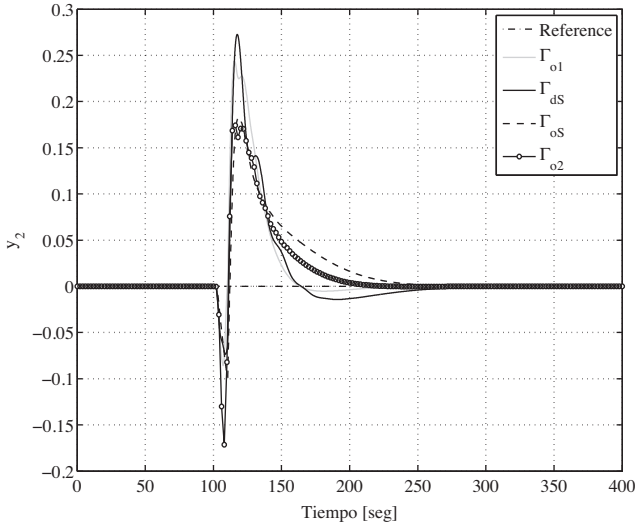

(b) Side composition-y_2

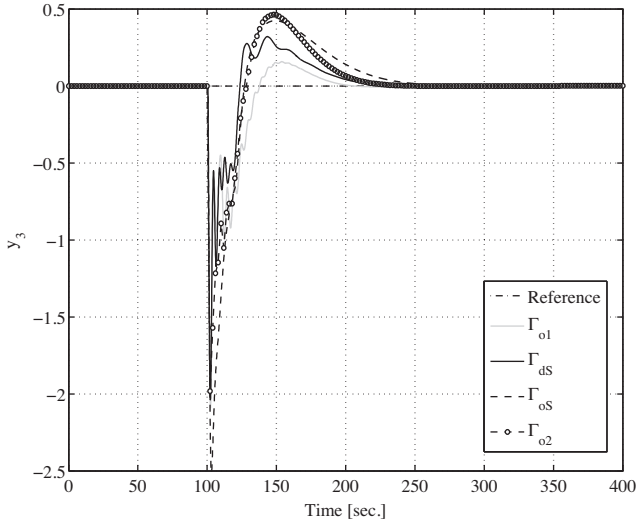

(c) Stage 19 temperature-y_3

Fig. 7. OR process – regulator profiles. (a) Top composition-y_1; (b) side composition-y_2; and (c) stage 19 temperature-y_3.

Table 7
OR process – IAE indexes.

Γ	Servo	Regulator
Γ_{o1}	140.70	35.39
Γ_{dS}	142.60	38.24
Γ_{o2}	149.40	51.45
Γ_{oS}	195.30	63.05

The best performances are highlighted with gray background.

Section 2.2 (Note 3) can be demonstrated here since the best servo performance corresponds to the full structure. The servo scenario is simulated with sequential unitary step changes in references at $t = 0$, 200, and 400 s for y_1, y_2 and y_3 respectively with a total simulation time of 600 s.

In this case, the full control structure has the best performance in both servo and regulator scenarios. In fact, Γ_{o1} improves the Γ_{oS}-based strategy with ≈28% and ≈44% respectively.

Table 8
CL process model.

	$\mathbf{G}_s(s)$				$\mathbf{D}_s(s)$
	u_1	u_2	u_3	u_4	d_1
y_1	$\frac{4.45}{(14s+1)(4s+1)}$	$\frac{-7.4}{(16s+1)(4s+1)}$	0	$\frac{0.35}{(25.7s+1)(2s+1)}$	$\frac{1.02e^{-4.5s}}{(25s+1)(2s+1)^2}$
y_2	$\frac{17.3e^{-0.9s}}{(17s+1)(0.5s+1)}$	$\frac{-41}{(21s+1)(s+1)}$	0	$\frac{9.2}{(20s+1)}$	$\frac{19.7e^{-0.3s}}{(25s+1)(s+1)}$
y_3	$\frac{0.22e^{-1.2s}}{(17.5s+1)(4s+1)}$	$\frac{-4.66}{(13s+1)(4s+1)}$	$\frac{3.6}{(13s+1)(4s+1)}$	$\frac{0.042(78.7s+1)}{(21s+1)(11.6s+1)(3s+1)}$	$\frac{0.75e^{-5s}}{(15.6s+1)(2s+1)^2}$
y_4	$\frac{1.82e^{-s}}{(21s+1)(s+1)}$	$\frac{-34.5}{(20s+1)(s+1)}$	$\frac{12.2e^{-0.9s}}{(18.5s+1)(s+1)}$	$\frac{-6.92e^{-0.6}}{(20s+1)}$	$\frac{16.1e^{-0.6s}}{(25s+1)(2s+1)}$

3.2.2. Chiang and Luyben process

This case study, also called CL process (Chang & Yu, 1994), represents two feed-split heat-integrated distillation columns for methanol-water separation. The simplified open-loop model of the plant represents a 4×4 square control problem as it is shown in Table 8, and has the following description: y_1 and y_2 top and bottom composition in the high pressure column, y_3 and y_4 top and bottom composition in the low pressure column, u_1 and u_2 reflux flow and heat input in the high pressure column, u_3 reflux flow in the low

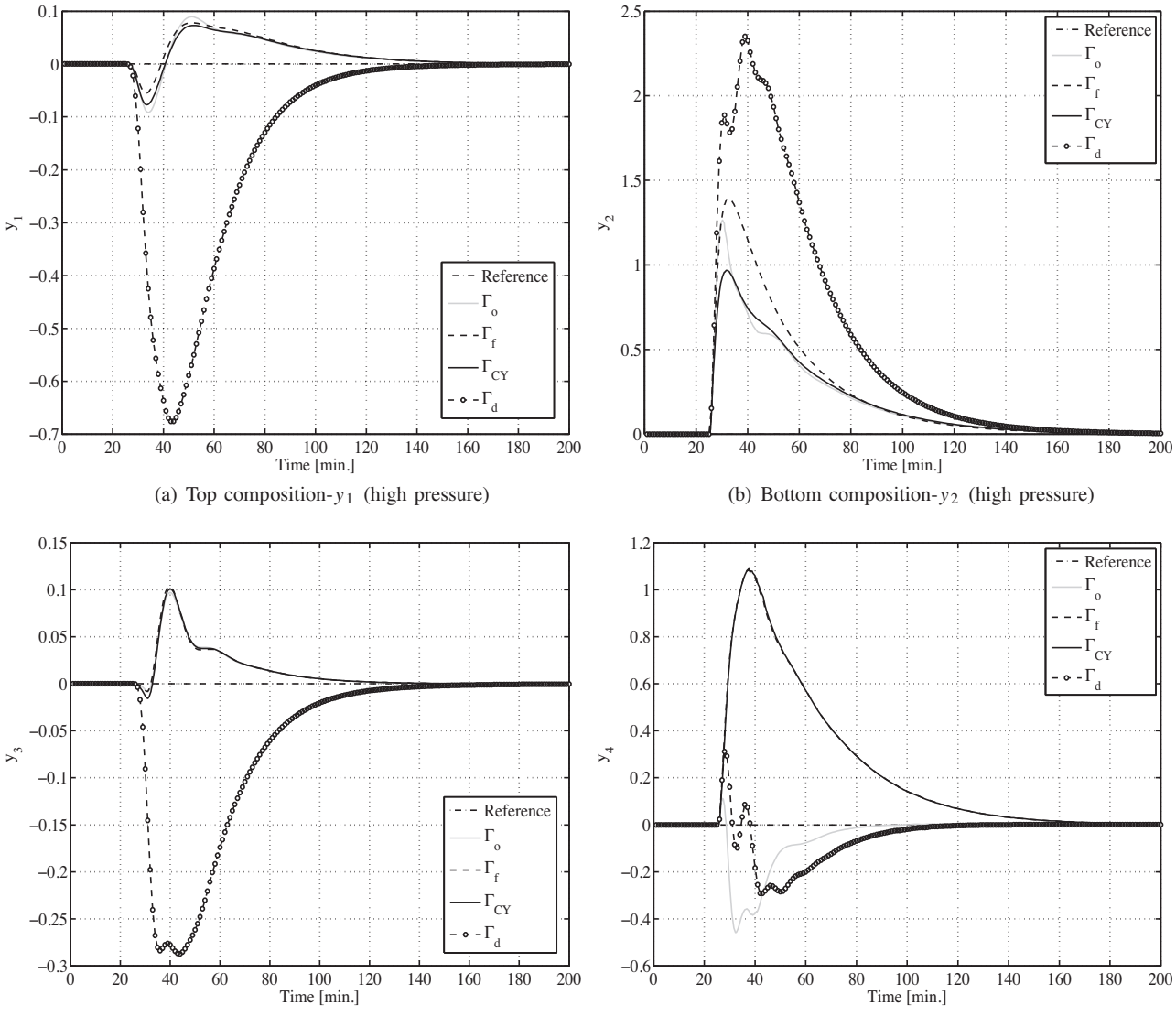

(a) Top composition-y_1 (high pressure)

(b) Bottom composition-y_2 (high pressure)

(c) Top composition-y_3 (low pressure)

(d) Bottom composition-y_4 (low pressure)

Fig. 8. CL process – regulator profiles. (a) Top composition - y_1 (high pressure); (b) bottom composition - y_2 (high pressure); (c) top composition - y_3 (low pressure); and (d) bottom composition - y_4 (low pressure).

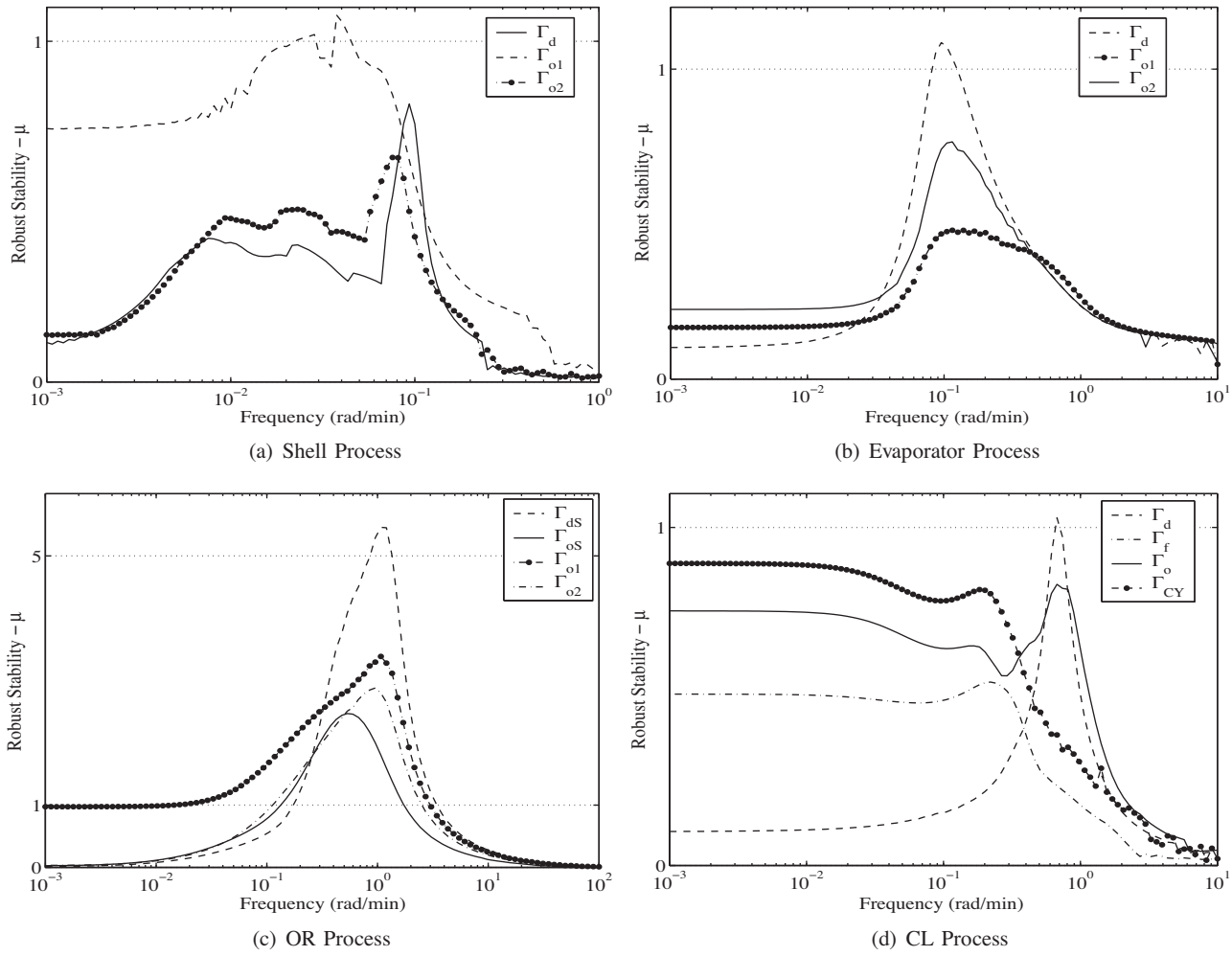

Fig. 9. Robust stability (μ-analysis). (a) Shell process; (b) Evaporator process; (c) OR process; and (d) CL process.

pressure column, and u_4 the feed split. The feed composition is the disturbance, d_1 (see Appendix B, Fig. 10(d)).

The pairings suggested by RGA and RNGA approaches are the same: $u_1 - y_1$, $u_2 - y_2$, $u_3 - y_3$, and $u_4 - y_4$ as preliminary decentralized control strategy. So, the following evaluation is the NLE approach via Eq. (21) with the parametrization suggested in Section 2.2.1, thus the combinatorial problem to be solved has $4^{(4\times4-4)} = 4096$ potential solutions and can be evaluated exhaustively. In this case an equally weighting with $\Delta_1 = \mathbf{I}_4$, $\Delta_2 = \mathbf{I}_4$, $\Xi_1 = 1$ and $\Xi_2 = \mathbf{I}_4$, is proposed. This setting generates the optimal model selection called Γ_o as it is shown in Eq. (30). Clearly, this parametrization gives a sparse control structure. Moreover, three alternative model selections are suggested for comparison purposes: Γ_d representing a decentralized control policy, Γ_f which represents a controller with full interaction, and the optimal sparse control structure (almost triangular) opportunely proposed by Chang and Yu (1990) and called here Γ_{CY}. All these proposals are compared via dynamic simulations in Fig. 8.

$$\Gamma_o = \begin{bmatrix} 1 & 1 & 0 & 0 \\ 1 & 1 & 0 & 0 \\ 1 & 1 & 1 & 0 \\ 0 & 0 & 0 & 1 \end{bmatrix} \quad \Gamma_d = \begin{bmatrix} 1 & 0 & 0 & 0 \\ 0 & 1 & 0 & 0 \\ 0 & 0 & 1 & 0 \\ 0 & 0 & 0 & 1 \end{bmatrix} \quad \Gamma_f = \begin{bmatrix} 1 & 1 & 1 & 1 \\ 1 & 1 & 1 & 1 \\ 1 & 1 & 1 & 1 \\ 1 & 1 & 1 & 1 \end{bmatrix} \quad \Gamma_{CY} = \begin{bmatrix} 1 & 1 & 0 & 0 \\ 1 & 1 & 0 & 0 \\ 1 & 1 & 1 & 0 \\ 1 & 1 & 1 & 1 \end{bmatrix} \tag{30}$$

Table 9
CL process – IAE indexes.

Γ	Servo	Regulator
Γ_f	35.97	94.97
Γ_{CY}	46.09	85.54
Γ_o	58.55	51.25
Γ_d	74.64	138.70

The best performances are highlighted with gray background.

Fig. 8 shows the CL process behavior in closed-loop when the controllers suggested by Eq. (30) are implemented. A regulator scenario is proposed with an unit step change at $t = 25$ min for $d_1(s)$. In this context, the optimal solution (Γ_o) given by the NLE-based CSD approach has the best performance and the structure suggested by Chang and Yu (1990) (Γ_{CY}) the second best, as is shown in Table 9. In addition, the full and decentralized (Γ_f and Γ_d) controller structures have the worst regulator performances in this scenario. Moreover, accounting again Table 9, the total IAE for the servo behavior can be evaluated. In this case, unitary step changes in each reference are proposed at $t = 0$, 100, 200, and 300 min for y_1, y_2, y_3 and y_4 respectively with a total simulation time of 400 min. Again here

and consistent with conclusion stated in Section 2.2 (Note 3) the best servo performance corresponds to the full structure (Γ_f).

In this case, CL process, the full control structure improves both the servo and regulator performance about ≈52% and ≈32% respect to the decentralized case respectively. Similarly, the optimal solution proposed here (Γ_o-based controller) suggests an improvement of ≈22% and ≈63% for the same scenarios. In conclusion, all control structures with some degree of interaction (presented here) significantly improves the dynamic behavior.

3.3. Robust stability test: μ-analysis

Control structures proposed in Sections 3.1 and 3.2 for each case study are evaluated and tested here by using the robust stability concepts. Particularly, the SSV or μ-analysis is used to quantify the robustness degree. Both parametric and unmodeled dynamic (multiplicative input) uncertainties were proposed for all delays and input gains of the process respectively. It is important to note that conclusions obtained from μ-analysis are directly tied to the considered perturbation structure.

Fig. 9 summarizes the μ indexes for robust stability (RS) analysis for all process and control structures suggested opportunely. A 20% of parametric uncertainty was selected for each dead time component in all TFMs. A complex perturbation was proposed as multiplicative input uncertainty. This approach is useful for considering gain perturbations generated by actuators, normally tied to the frequency. Thus, a complex perturbation with gain variations between 10% at steady-state to 200% at high frequency is proposed for the Shell, Evaporator and CL processes. The remaining case, OR, is more sensitive to this uncertainty and was analyzed with 1% at steady-state to 5% at high frequency as a complex gain perturbation.

Fig. 9(a) shows the closed-loop behavior of the Shell process when different control structures are used. In fact, optimal solution Γ_{o1} does not guarantee RS ($\max(\mu)>1$) with the proposed perturbation structure. On the other hand, decentralized (Γ_d) and sparse controller (Γ_{o2}) have similar good behaviors ensuring RS. Fig. 9(b) displays the evaporator μ profiles when several control structures are used. In this case, decentralized (Γ_d) approach does not guarantee RS, instead optimal proposals called Γ_{o1} (full) and Γ_{o2} (sparse) ensure a good RS degree. In fact, full structure presents the lowest peak value in μ. The OR process is analyzed in Fig. 9(c). Although the multiplicative uncertainty has been reduced in magnitude, the closed-loop process still having serious problems to ensure RS, regardless of control structure. In fact, all closed loop systems present peaks in μ greater than 1. The worst case is given by the decentralized approach tuned by Shen et al. (2010) recommendation, Γ_{dS}. Fig. 9(d) summarizes the μ profiles for CL process and their corresponding control structures. It is clear that decentralized approach, Γ_d, does not guarantee RS and sparse structure suggested by Chang and Yu (1992), Γ_{CY}, is very close to the RS limit. On the other hand, the sparse control approach suggested here and the full case present a good RS limits, and particularly Γ_f has the best performance, lowest $\max(\mu)$.

4. Conclusions and future work

In this work the MSD approach was applied successfully in several well-tested case studies and compared with other approaches for plant-wide control design. It was demonstrated through this procedure that decentralized and full control policies are not always the best solution, either from performance and/or robust stability point of view. Moreover, relevant conclusions have been obtained about the best control structure for servo behavior. In fact, the full control structure is the best choice for that goal (in all cases gave the lowest IAE magnitude). On the other hand, for a specific sparse controller structure the regulator behavior can be significantly improved at the expense of the servo behavior. It is caused by the trade-off between servo and regulator requirements. Even though the MSD approach tries to reduce the use of heuristic considerations, the best CVs selection and controller structure must be analyzed in the context of each particular process and their needs (original control requisites). In this first stage the MSD strategy was developed to address the non-square process with more outputs than inputs (Optimal CVs selection), but in future works an optimal manipulated variables selection (OMS) approach will be included to the MSD for complementing the procedure. Moreover, future developments also consider the integration of the MSD approach to process synthesis stage and fault-tolerant control design, for example. Finally, an important challenger is to test this approach on a larger case, such as the pulp mill process (Castro & Doyle, 2004) to achieve a realistic perception of its potentiality.

Acknowledgements

The authors thank the financial support of CONICET (Consejo Nacional de Investigaciones Científicas y Técnicas) and ANPCYT (Agencia Nacional de Promoción Científica y Técnica) from Argentina. The authors also acknowledge the support of the UTN-FRRo.

Appendix A. Tuning: all case studies

The controller tuning information used for each control policy is summarized here. Accounting the tuning rules stated in Section 2.3, considering $k_{ij}^m/(1+\tau_{ij}^m s)$ as the ij component of $\tilde{\mathbf{G}}_{s\Gamma}^-$, θ_{ij} is the dead time for the ij component in the FOPD approximation of the process,

Table 10
Filter time constants – all case studies.

Process	Structures	τ_{f1}	τ_{f2}	τ_{f3}	τ_{f4}
Shell	Γ_d	$\theta_1^{max}+15$	$\theta_2^{max}+15$	$\theta_3^{max}+7$	–
	Γ_{o1}	$\theta_{11}+10$	$\theta_{22}+10$	$\tau_{33}^m/2$	–
	Γ_{o2}	$\theta_{11}+10$	$\theta_{22}+10$	$\tau_{33}^m/2$	–
Evaporator	Γ_d	$5\theta_{11}$	$5\theta_{22}$	–	–
	Γ_{o1}	$5\theta_{11}$	$5\theta_{22}$	–	–
	Γ_{o2}	$5\theta_{11}$	$5\theta_{22}$	–	–
OR	Γ_{o1}	$3.8\theta_{11}$	$3\theta_{22}$	$1.5\theta_{33}$	–
	Γ_{o2}	$3.8\theta_{11}$	$3\theta_{22}$	$1.5\theta_{33}$	–
	Γ_{dS}	Suggested by Shen et al. (2010)			–
	Γ_{oS}	Suggested by Shen et al. (2010)			–
CL	Γ_o	$\theta_1^{max}+1$	$\theta_2^{max}+2$	$\theta_3^{max}+1.5$	$\theta_4^{max}+1.1$
	Γ_d	$\theta_1^{max}+1$	$\theta_2^{max}+2$	$\theta_3^{max}+1.5$	$\theta_4^{max}+1.1$
	Γ_f	$\theta_1^{max}+1$	$\theta_2^{max}+2$	$\theta_3^{max}+1.5$	$\theta_4^{max}+1.1$
	Γ_{CY}	Suggested by Chang and Yu (1990)			

and the stability/robustness condition at Eq. (22), so, a conservative tuning is proposed such as: $\tau_{fi} \geq \max_j(\theta_{ji}) = \theta_i^{max}$, with $j = 1, \ldots, n$. In all cases presented here the $\tilde{\mathbf{G}}_{s\Gamma}^{-}$ component was selected from the FOPD process model without consider the corresponding delays.

The filter time constants, for all case studies, are displayed in Table 10. In the following paragraphs, some comments are given about the tuning methodology. For the Shell oil fractionator case $\tilde{\mathbf{G}}_{s\Gamma}^{-}$ was extracted from Table 1, which is a FOPD representation, by selecting first, second and seventh output. So, $\theta_1^{max} = 27$, $\theta_2^{max} = 28$, $\theta_3^{max} = 27$, $\theta_{11} = 27$, $\theta_{22} = 14$, and $\theta_{33} = 0$. Note that decentralized control policy was tuned conservatively because its inherent robustness problems. The tuning parameters for the Evaporator process were obtained considering the invertible part from a FOPD model (not given here) and $\theta_1^{max} = 5$, $\theta_2^{max} = 15$, $\theta_{11} = 5$, and $\theta_{22} = 1$. Note that τ_{f2} does not require a conservative tuning. The control policies for the Ogunnaike and Ray (OR) process were tuned accounting a FOPD approximation of the model in Table 6 and considering $\theta_1^{max} = 9.2$, $\theta_2^{max} = 9.4$, $\theta_3^{max} = 1.2$, $\theta_{11} = 2.6$, $\theta_{22} = 3$, and $\theta_{33} = 1$. The next case is the Chiang and Luyben (CL) process. It is also considered a FOPD approximation of the model in Table 8 to develop the invertible part. Moreover, $\theta_1^{max} = 2.5$, $\theta_2^{max} = 0.3$, $\theta_3^{max} = 1.5$, $\theta_4^{max} = 1.5$, $\theta_{11} = 1.5$, $\theta_{22} = 0.3$, $\theta_{33} = 1$, and $\theta_{44} = 0.6$.

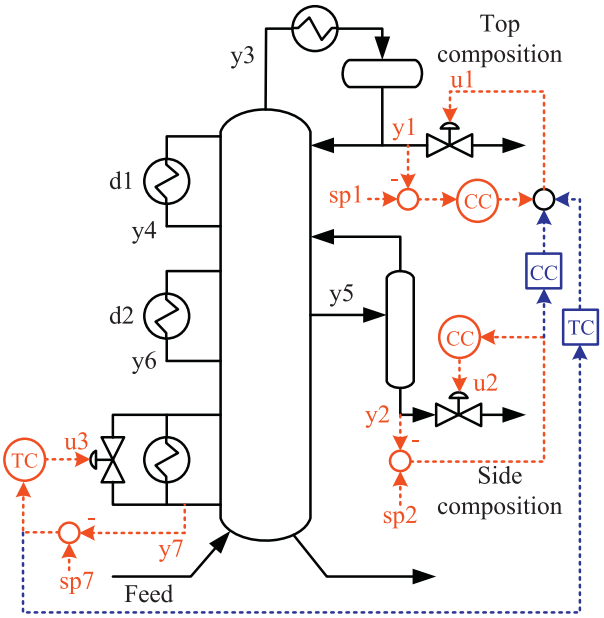

(a) Shell process and CS Γ_{o2}

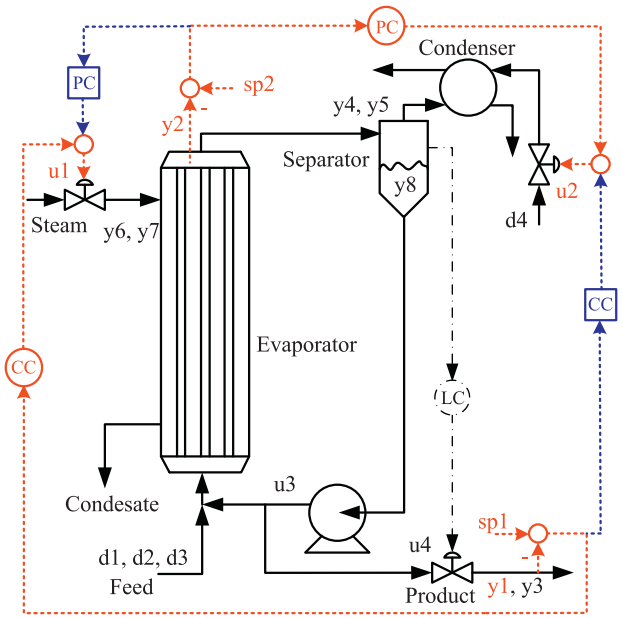

(b) Evaporator process and CS Γ_{o1}

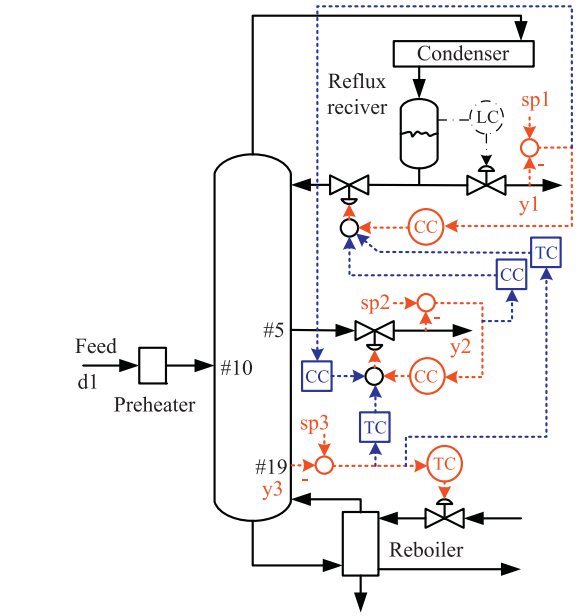

(c) OR process and CS Γ_{o2}

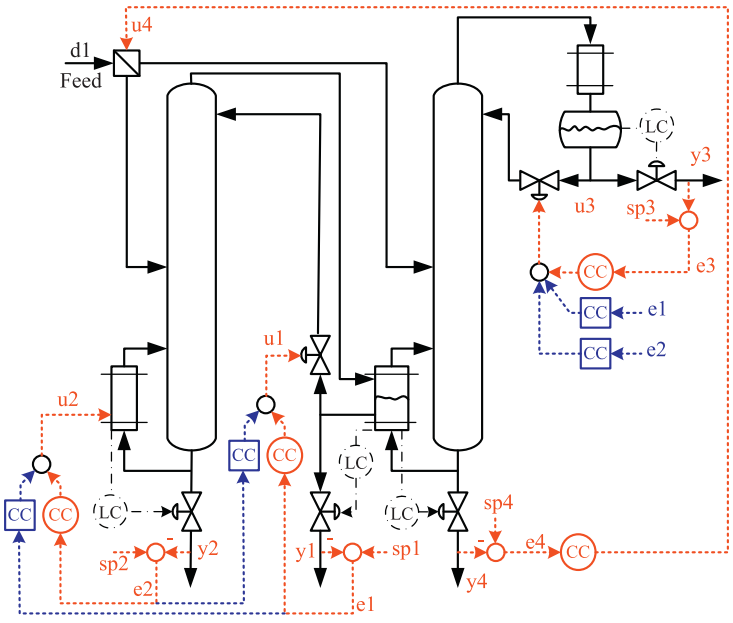

(d) CL process and CS Γ_o

Fig. 10. Case studies and control structures. (a) Shell process and CS Γ_{o2}; (b) Evaporator process and CS Γ_{o1}; (c) OR process and CS Γ_{o2}; and (d) CL process and CS Γ_o.

Appendix B. Selected control structures

In this section, the process layout and its corresponding control structure (CS) is given for the case studies considered. In fact, Fig. 10(a)–(d) displays the Shell oil fractionator, the Newell and Lee evaporator, the OR process, and the CL integrated columns schemes. The final plant-wide control policies were derived from the analysis performed in Sections 3 and 3.3. The selected control structures are: Γ_{o2} from Eq. (27), Γ_{o1} from Eq. (28), Γ_{o2} from Eq. (29), and Γ_o from Eq. (30), respectively. Note that, the dash–dot lines refer to level controllers, the red-dashed lines and circles represent diagonal control loops, and the blue-dashed lines and squares summarize the optimal interaction given by the NLE approach.

References

Assali, W., & McAvoy, T. (2010). Optimal selection of dominant measurements and manipulated variables for production control. *Industrial & Engineering Chemistry Research*, *49*, 7832–7842.

Bristol, E. (1966). On a new measure of interaction for multivariable process control. *IEEE Transactions on Automatic Control*, *11*(1), 133–134.

Buckley, P. (1964). *Techniques of process control*. New York, USA: Willey.

Castro, J., & Doyle, F. (2004). A pulp mill benchmark problem for control: Problem description. *Journal of Process Control*, *14*, 17–29.

Chang, J., & Yu, C. (1990). The relative gain for non-square multivariable systems. *Chemical Engineering Science*, *45*, 1309–1323.

Chang, J., & Yu, C. (1992). Relative disturbance gain array. *AIChE Journal*, *38*, 521–534.

Chang, J., & Yu, C. (1994). Synthesis of controller structures for robust load performance. *International Journal of Control*, *60*, 1353–1369.

Garcia, C., & Morari, M. (1985). Internal model control. 2. Design procedure for multivariable systems. *Industrial & Engineering Chemistry Process Design and Development*, *24*, 472–484.

Golub, G., & Van Loan, C. (1996). *Matrix computations*. (3rd ed.). Baltimore, Maryland, USA: Johns Hopkins University Press.

Govatsmark, M., & Skogestad, S. (2001). Control structure selection for an evaporation process. *European Symposium on Computer Aided Process Engineering*, *11*, 657–662.

Grosdidier, P., Morari, M., & Holt, B. (1985). Closed-loop properties from steady-state gain information. *Industrial & Engineering Chemistry Fundamentals*, *24*, 221–235.

He, M., Cai, W., Ni, W., & Xie, L. (2009). RNGA based control system configuration for multivariable processes. *Journal of Process Control*, *19*, 1036–1042.

Hori, E., & Skogestad, S. (2008). Selection of controlled variables: Maximum gain rule and combination of measurements. *Industrial & Engineering Chemistry Research*, *47*, 9465–9471.

Hori, E., Skogestad, S., & Alstad, V. (2005). Perfect steady-state indirect control. *Industrial & Engineering Chemistry Research*, *44*, 863–867.

Horn, R., & Johnson, C. (1990). *Matrix analysis*. Cambridge University Press.

Kariwala, V., & Cao, Y. (2010a). Bidirectional branch and bound for controlled variable selection. Part III: Local average loss minimization. *IEEE Transactions on Industrial Informatics*, *6*, 54–61.

Kariwala, V., & Cao, Y. (2010b). Branch and bound method for multiobjective pairing selection. *Automatica*, *5*, 932–936.

Khaki-Sedigh, A., & Moaveni, B. (2009). *Control configuration selection for multivariable plants*. Berlin, Heidelberg: Springer-Verlag.

Lin, F., Jeng, J., & Huang, H. (2009). Multivariable control with generalized decoupling for disturbance rejection. *Industrial & Engineering Chemistry Research*, *48*, 9175–9185.

Ljung, L. (1999). *System identification: Theory for the user* (2nd ed.). New Jersey, USA: Prentice Hall.

Luyben, W. (1986). Simple method for tuning SISO controllers in multivariable systems. *Industrial & Engineering Chemistry Process Design and Development*, *25*, 654–660.

Luyben, W., Tyréus, B., & Luyben, M. (1998). *Plant-wide process control*. New York, USA: McGraw-Hill.

Maciejowski, J. (2002). *Predictive control with constraints*. Harlow, Essex, England: Prentice Hall.

McAvoy, T., Arkun, Y., Chen, R., Robinson, D., & Schnelle, P. (2003). A new approach to defining a dynamic relative gain. *Control Engineering Practice*, *11*, 907–914.

Molina, G., Zumoffen, D., & Basualdo, M. (2009). A new systematic approach to find plantwide control structures. *Computer Aided Chemical Engineering*, *27*, 1599–1604.

Molina, G., Zumoffen, D., & Basualdo, M. (2011). Plant-wide control strategy applied to the Tennessee Eastman process at two operating points. *Computers & Chemical Engineering*, *35*, 2081–2097.

Monica, T., Yu, C., & Luyben, W. (1988). Improved multiloop single-input/single-output (SISO) controllers for multivariable processes. *Industrial & Engineering Chemistry Research*, *27*, 969–973.

Shen, Y., Cai, W., & Li, S. (2010). Multivariable process control: Decentralized, decoupling or sparse? *Industrial & Engineering Chemistry Research*, *49*, 761–771.

Skogestad, S., & Postlethwaite, I. (2005). *Multivariable feedback control. Analysis and Design*. Chichester, West Sussex, England: John Wiley & Sons.

Skogetad, S., & Morari, M. (1987). Implications of large RGA elements on control performance. *Industrial & Engineering Chemistry Research*, *26*, 2323–2330.

Yuan, Z., Chen, B., & Zhao, J. (2011). Effect of manipulated variables selection on the controllability of chemical processes. *Industrial & Engineering Chemistry Research*, http://dx.doi.org/10.1021/ie2001132

Zumoffen, D., & Basualdo, M. (2009). Optimal sensor location for chemical process accounting the best control configuration. *Computer Aided Chemical Engineering*, *27*, 1593–1598.

Zumoffen, D., & Basualdo, M. (2010). A systematic approach for the design of optimal monitoring systems for large scale processes. *Industrial & Engineering Chemistry Research*, *49*, 1749–1761.

Zumoffen, D., Molina, G., Nieto, L., & Basualdo, M. (2011). Systematic control approach for the Petlyuk distillation column. *18th IFAC World Congress*, 8552–8557.